OCEANS AND ATMOSPHERE FLAGSHIP
www.csiro.au

Remote sensing methods to map and monitor the condition of coastal habitats and other surrogates for biodiversity

Part A: Floodplain vegetation mapping of the Kakadu National Park

Janet M. Anstee, Elizabeth J. Botha, Guy T. Byrne, Peter Dyce and Thomas Schroeder

Image Processing and Analysis Report

March 2015
Prepared for the NERP Northern Australia Hub

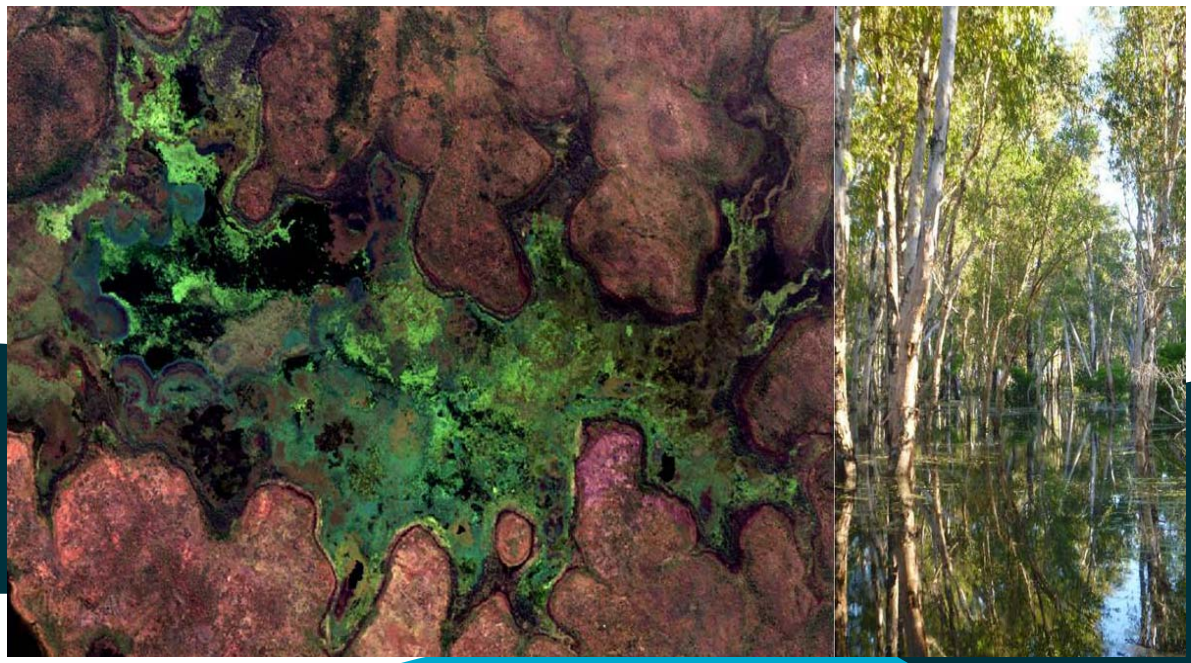

National Environmental Research Program

Citation

Anstee, J.M, Botha, E.J., Byrne, G.T., Dyce, P. and Schroeder, T. (2015) Remote sensing methods to map and monitor the condition of coastal habitats and other surrogates for biodiversity, Part A: Floodplain vegetation mapping of the Kakadu National Park, CSIRO Oceans & Atmosphere Flagship, Australia.

Copyright and disclaimer

Important disclaimer

Cover photographs

Left: Boggy Plain Kakadu National Park (KNP) observed with WorldView-2, Right: Magela floodplain KNP.

Contents

Figures

Tables

1 Executive Summary

This report describes the results of applying remote sensing methods to floodplain vegetation monitoring in Kakadu National Park, NT.

Visualising the spatial distribution of aquatic benthic habitats is essential to our understanding of these ecosystems and to our ability to provide early management intervention. This requires objective, repeatable processing pathways of earth observation data. Therefore, this project undertook the following activities:

- Acquired recent medium and high resolution images with the long term goal of identifying change over time.
- Analysed medium and high resolution images and other ancillary data sources (eg LiDAR) and applied spectral analysis techniques developed for the Kakadu floodplains.

  This included:
  - Application of a geophysical approach to measurements and modeling of the image
  - Separation of tree and below canopy layers.
  - Generation of object-oriented classifications of floodplain vegetation distribution.
  - Validation of the satellite imagery based analysis results with all available field data.

These activities, producing and assessing the satellite derived maps, led to an improved understanding about current floodplain vegetation distribution.

The geographic object-oriented image analysis (GEOBIA) approach employed resulted in a better delineation of the vegetation beds and the fuzzy c-means classification produced less speckled classification results compared to traditional per-pixel based classification methods. The overall accuracy of the floodplain vegetation classification results were 64% and 26% for the ALOS South Alligator and Magela images and 87% and 88% for the WorldView2 Boggy Plains 2010 and 2012 images.

The available field data, although high quality for the purpose for which it was acquired, was not sufficient for accurate assessment of the satellite derived vegetation maps.

The resultant ALOS and WorldView2 floodplain vegetation maps produced provide a spatially dense picture of floodplain vegetation coverage in floodplains of the Kakadu NP and are available on CSIRO Data Access Portal (DAP) for collaborators to use.

2 Introduction

There is a paucity of biological data across the remote and inaccessible northern Australian coastline that currently constrains bioregional planning processes, development approvals and, ultimately, the conservation of biodiversity. The natural resource management of the Alligator Rivers Region encompassing Kakadu National Park relies on long-term monitoring of key biophysical parameters in the wetlands and adjacent seas where often little is known about biodiversity and ecosystem processes. Areas that are potential transitional or habitat refugia in the face of climate change should be identified and mapped (Keppel et al. 2012).

The first step in mapping and monitoring these ecosystems is to provide baseline maps that document the current extent, diversity and condition of habitat. The next step is to establish monitoring programs designed to detect disturbance at an early stage, and to distinguish such disturbance from natural variation (Kirkman 1996, Kendrick et al. 2000, Borum et al. 2004).

Historically, mapping and assessment at a habitat-scale has been undertaken through the use of aerial photographic interpretation (API) and direct field mapping - a labour intensive and somewhat subjective assessment methodology. Field methods, such as transects and point-observations (Norris et al. 1997, Norris and Wyllie-Echeverria 1997), produce mapping errors due to the need for spatial interpolation between the *in situ* data points or transects.

Increasingly, remote sensing techniques have been adopted as an alternative method due to the combined development of sensor sophistication (such as higher spectral, spatial, radiometric and temporal resolution) and image classification tools, such as geographic object based image analysis (GEOBIA). The use of advanced satellite and /or airborne remote sensing technologies also provides an opportunity to undertake more cost effective and objective monitoring (Duarte et al. 2004, Dekker et al. 2006 and Dekker et al. 2008). Multi-date satellite remote sensing is geographically highly repeatable and a cost effective method for detecting large changes in habitat status or extent over time (Macleod and Congalton 1998).

Specifically this project aims to:

(1) Map the extent and type of vegetation of the South Alligator Rivers floodplain using multispectral very high spatial resolution satellite imagery;
(2) Apply advanced image processing techniques such as atmospheric correction, field spectroradiometry and OBIA classification to high resolution imagery, in an innovative, repeatable, objective manner.

2.1 Project objectives

Visualising the spatial distribution of wetland habitats is essential to our understanding of the wetland ecosystems and to our ability to provide early management intervention. This requires objective, repeatable processing pathways of earth observation data. Therefore, this project undertook the following activities designed to improve the accuracy of the information:

- Acquired recent medium (ALOS-AVNIR) and high resolution (WorldView-2) images to establish habitat baselines.
- Analysed medium and high resolution images and other ancillary data sources (e.g. LiDAR and inundation frequency datasets) and applied spectral analysis techniques developed for the Alligator Rivers floodplains.
  This included:
    - Application of an atmospheric correction technique.
    - Generation of object-oriented classifications of floodplain vegetation distribution.
    - Separation of tree and sub-canopy layers.
    - Separation of dry/saline areas from frequently inundated areas.
    - Calibration of the satellite imagery based analysis results with all available field data.

3 Data Acquisition

The ALOS (Advanced Land Observation Satellite) was launched in 2006 with the PRISM, PALSAR and AVNIR sensors onboard and represents an intermediate spatial resolution satellite image at 10 m resolution for the AVNIR sensor (Table 1). The planned operational lifetime was three years, in a near-polar, sun-synchronous orbit, at a mean altitude of 691 km. It was operational until 2011.

Table 1 Spectral Characteristics of ALOS AVNIR-2 sensors, from http://www.eorc.jaxa.jp/ALOS/en/about/avnir2.htm

AVNIR-2	Lower Band Edge (nm)	Centre Wavelength (nm)	Higher Band Edge (nm)
Blue	420	460	500
Green	520	560	600
Red	610	650	690
Near-IR 2	760	825	890

The WorldView-2 (WV2) high-resolution commercial imaging satellite was launched in 2009. The satellite is in a nearly circular, sun-synchronous orbit at an altitude of approximately 770 km. WV2 imagery has a high spectral resolution (Table 2), a 2m spatial resolution and therefore offers the best potential for vegetation assessment.

Table 2 Spectral Characteristics of WorldView-2 sensors, from http://www.digitalglobe.com/sites/default/files/DigitalGlobe_Spectral_Response_0.pdf

WorldView-2	Lower Band Edge (nm)	Centre Wavelength (nm)	Higher Band Edge (nm)
Coastal Blue	396	427	458
Blue	442	478	515
Green	506	546	586
Yellow	584	608	632
Red	624	659	694
Red Edge	699	724	749
Near-IR 1	765	833	901
Near-IR 2	856	949	1043

Limited coverage of ALOS and WV2 satellite imagery was available for the study location, but with the existing data, a selection was made based on the following considerations to ensure the optimal image purchase (Held et al. 2003):

1. **Atmospheric conditions:** Atmospheric effects, such as variable haze and smoke and cloud and cloud shadows, are difficult to correct for. Although the satellite image provider estimates cloud cover, this automated assessment is not always accurate, especially when the image includes high amounts of atmospheric haze. Therefore all images have to be visually assessed before purchase to ensure suitable quality.
2. **Sun-sensor geometry:** The angular relationships between the sun, the object and the sensor, cause differences in the bidirectional reflectance of the object and can significantly affect the reflectance of objects in an image. The ultimate impact of the sun-senor geometry is that it can affect object discrimination and hence classification accuracy. For example, if the sensor is only viewing the sunlit portion of an object without any shadowing, this can significantly increase the reflectance value of that object (hot spot) while the same object will appear darker if the sensor view angle differs from the sun angle. The extreme pointing capability of some satellite sensors (e.g. up to 45 degree off nadir for WorldView-2) increases the possibility of the sensor imaging hot spots on land

or sun glint over water. Therefore, acquisition thresholds were applied when purchasing the imagery to ensure optimal viewing geometry of the satellite.

3. **Seasonality:** Seasonal variability in the growth cycles of weeds and native vegetation can affect the ability to discriminate different vegetation types. In order to effectively capture the extent and density of land cover classes, image acquisition should be tasked during periods of optimal vegetation cover. To ensure consistent change analysis, future image acquisitions should be tasked during the same season as that of the original baseline data
4. **Spatial Resolution:** Finer spatial resolution leads to higher data acquisition and processing costs. Accuracy is also improved with finer scale resolution with many airborne and satellite sensor systems providing very high positional accuracy due to the improvements in the use of inertial navigation systems and the integration of DEM information during the image geo-correction process. High levels of geo-spatial accuracy are essential when seeking to detect pixel-by-pixel changes (trend analysis).
5. **Spectral Resolution:** High spectral resolution improves the opportunities for aquatic macrophyte discrimination and assists in the sub-pixel identification of cover types (spectral un-mixing). Discrimination accuracy increases with improved spectral and spatial resolution. Figure 1 shows a vegetation spectrum taken *in situ*, then rescaled to the spectral resolution of 4 satellites (Landsat, ALOS-AVNIR2, QuickBird and WorldView-2) illustrating the degradation of the original spectral response with decreases in spectral and spatial resolution, impacting the discrimination accuracy.

The satellite image data that was eventually acquired is shown in Figure 2 and Table 3. A radar, Light Detection and Ranging (LiDAR) survey of the floodplains within Kakadu National Park conducted by Fugro Spatial Solutions for Geoscience Australia. The acquisition start date was the 22nd of October 2011 and the end date was the 16th of November 2011. The data supplied by Dr Renee Bartolo, Environmental Research Institute of the Supervising Scientist, Department of Environment.

The massive volume of point data collected from this survey was processed by Fugro Spatial Solutions into rasters in ESRI Grid™ format. There are 4941 Grids which form a tiled mosaic of the flood plains and estuaries of Kakadu National Park. The entire mosaic is geo-referenced and is stored on the CSIRO Data Access Portal (see Appendix A.5).

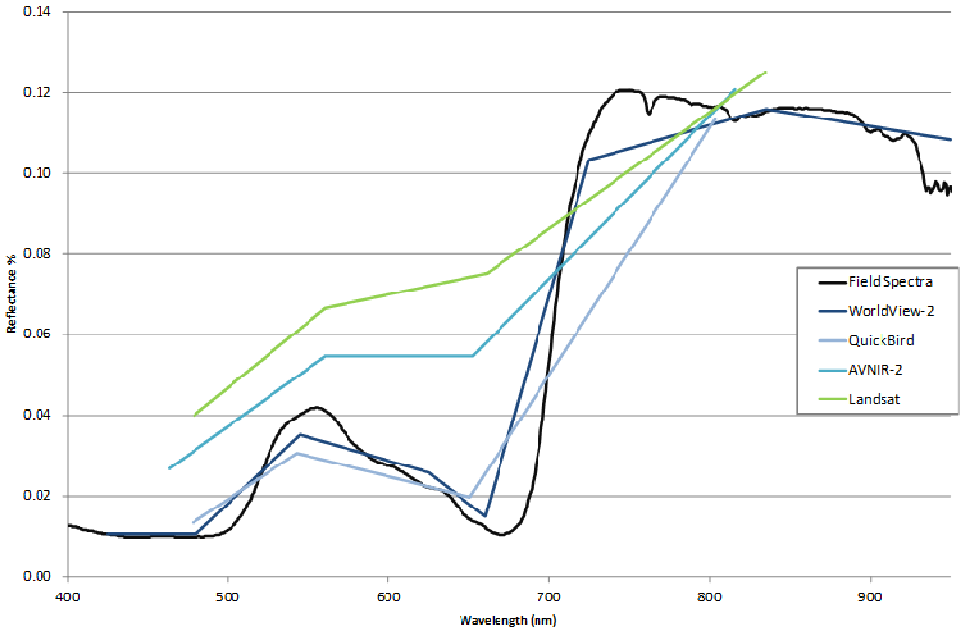

Figure 1: Example of the typical hyper-spectral response of green vegetation (field spectra) and the same spectrum translated to the expected multispectral response in WorldView-2, QuickBird, AVNIR-2 and Landsat spectral bands.

Table 3 Specifications of satellite image data acquired for processing

Area of interest	Acquisition Date	Sensor	Spatial resolution	Comments
South Alligator	13 May 2010	ALOS-AVNIR	10 m	reasonably high quality with a large smoke plume in the lower left of the imagery, bypassing most of the South Alligator and Magela floodplains
West Alligator	13 May 2010	ALOS-AVNIR	10 m	
Coastal Region	13 May 2010	ALOS-AVNIR	10 m	
Magela	13 May 2010	ALOS-AVNIR	10 m	
Boggy Plains	16 July 2010	WV2	2 m	very high quality with little atmospheric effects present, though some cloud shadowing is evident
Yellow Waters	16 July 2010	WV2	2 m	
Boggy Plains	6 June 2012	WV2	2 m	
Munmarlarly	6 June 2012	WV2	2 m	
Yellow Waters	6 June 2012	WV2	2 m	

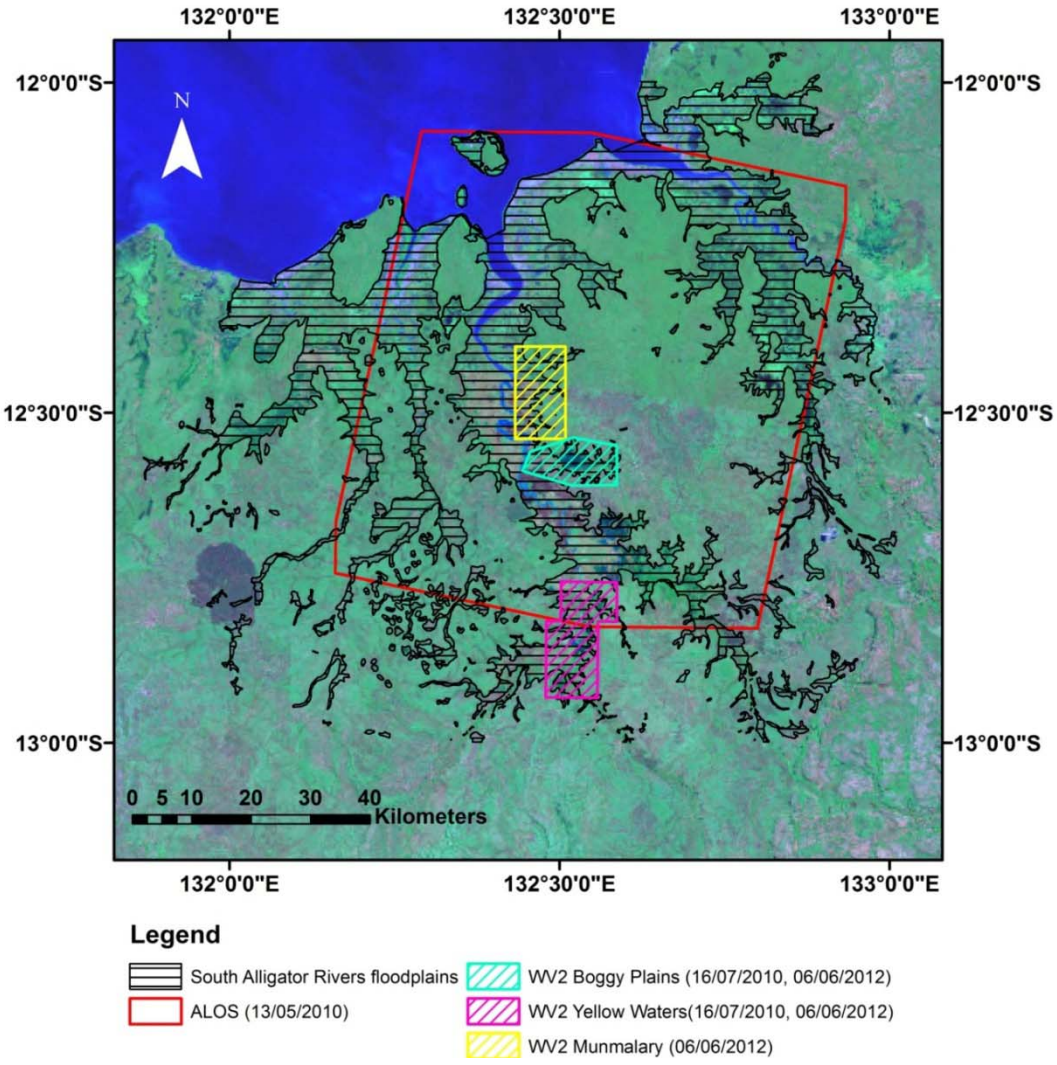

Figure 2 Location and extent of the ALOS and WV2 images acquired for processing within the Alligator Rivers Floodplains.

4 Image pre-processing

4.1 Geometric Correction

Geo-referencing of satellite images is required when combing the data with other forms of information such as field data. As we had acquired five WorldView-2 images for 3 areas (Figure 2), the images were co-registered where possible. The ALOS image was co-registered to the higher resolution WorldView-2 images. When comparing field data to the satellite data, some geometric discrepancies resulted in spatial offsets. To overcome this offset, accuracy assessment was only done on spatially homogeneous areas greater than 30m.

4.2 Atmospheric Correction

To ensure that the classified images can be compared to each other on a "like for like" basis, all the images were atmospherically corrected to represent surface reflectance. An atmospheric correction algorithm developed by CSIRO for application to coastal and inland water bodies, called the "coastal Water and Ocean MODTRAN-4 Based ATmospheric correction" ("c-WOMBAT-c") (Brando and Dekker, 2003), was applied to all images. c-WOMBAT-c applies a physics-based radiative transfer model to convert at-sensor radiance to apparent reflectance followed by an air-water interface correction to obtain the subsurface irradiance reflectance.

The atmospheric parameterization for each image was based on radiosonde data from the Australian Bureau of Meteorology Station at Jabiru to estimate the atmospheric column water content and the actual and 24 hour average wind speed. The estimate of Ozone content was downloaded for the dates of satellite overpasses from the Total Ozone Mapping Spectrometer (TOMS) database.

No concurrent *in situ* spectral data was available to assess the accuracy of the atmospheric correction applied to the imagery. For this reason, image reflectance data over pseudo-invariant features, such as paved roadways and bare ground, was collected over the same area in the images with different acquisition dates. These spectra were compared to each other to ensure that the surface reflectance retrieved by the atmospheric correction procedure is similar in both shape and albedo relative to each other (e.g. Figure 3). Closure of the atmospherically corrected imagery was assumed when the difference between the different dates was minimised.

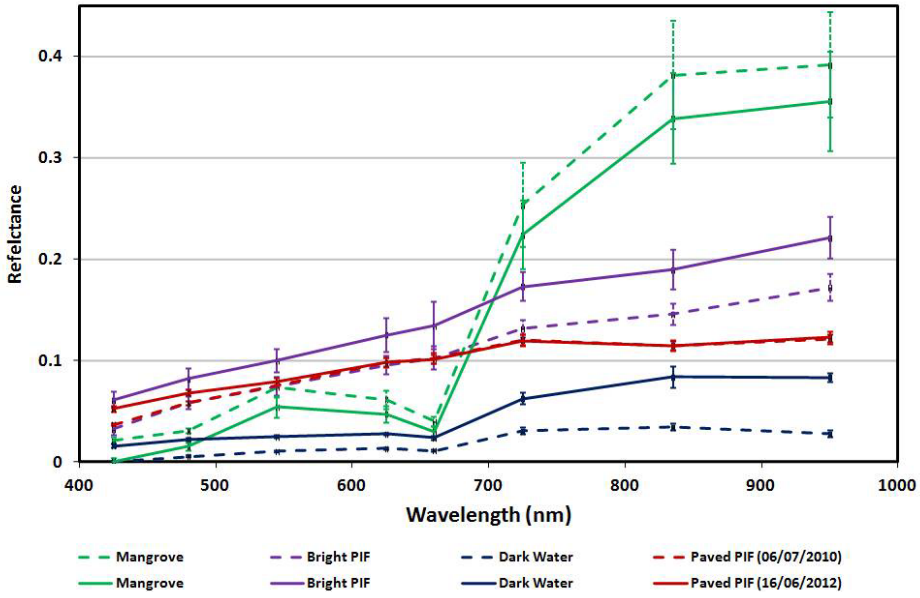

Figure 3 Example of the relative inter-comparison of pseudo-invariant features (PIF), collected from the Yellow Waters WV2 images acquired on 16/07/2010 and 06/06/2012, respectively.

5 Classification Methods – ALOS and WV2

The aim of this project was to make an assessment of the floodplain vegetation type distribution and produce maps locating coverage where they were visible in the ALOS and WV2 imagery. In addition to the satellite image data used for this purpose, elevation data, flood inundation frequency data (Ward et al. 2014) and local knowledge has been utilized to produce the most accurate maps possible from all available data. The LiDAR canopy height model was used to separate the trees from the sub-canopy in the satellite imagery. The sub-canopy images were further separated based on freshwater inundation frequency. Inundation frequency can be used as a surrogate of long term patterns of inundation duration. An interannual floodplain inundation extent product, produced from available Landsat data, captured at the end of the wet, season, mid-season and dry-season over a period spanning 22 years between 1988 and 2010 (Ward et al, 2014), delineated broad floodplain cover states which were utilised to separate the broad ecological classes within the imagery. A threshold of >7 (from a range of 1 to 17) was used for more frequently inundated wetter regions and <7 for the less frequently inundated. The 'wet' and 'dry' portions were compared with the field data as described in Table 4 and labelled accordingly. Figure 4 summarizes the workflow used to produce the final map products from these datasets.

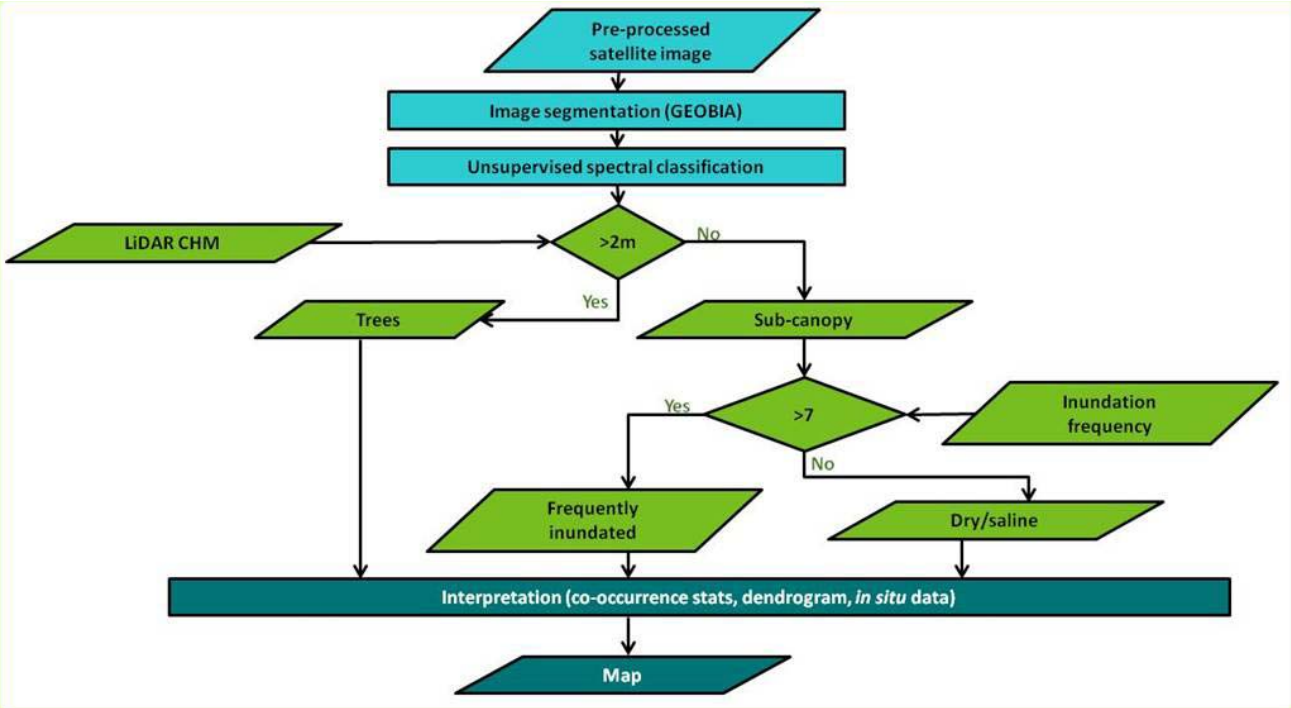

Figure 4 Flow-chart of the classification approach used to produce floodplain vegetation maps from the ALOS and WV2 images.

5.1 Image segmentation of ALOS and WV2 images

Geographic object-oriented-based image analysis (GEOBIA) and processing are valuable tools in preparing pixel-based image data for semi-automated classification. Unlike traditional pixel-based image analysis GEOBIA exploits the spatial and spectral relationships of elements of objects and cover types within the landscape. The use of differential band weightings and specific object scaling functions allow the inherent information (often visible to the human eye, but subtly expressed in the image data) to be more readily interpreted.

Preliminary investigations indicated that the images segmented into objects (through application of GEOBIA methods) prior to classification created more natural clusterings of the vegetation cover classes than per-pixel classifications. Hence, in this study, a novel semi-automated classification approach was applied, utilising both GEOBIA and traditional classification methods (Anstee and Byrne, 2014).

The atmospherically corrected ALOS and WV2 images were processed using a geographic object-oriented image analysis (GEOBIA) approach using the Trimble eCognition software (www.ecognition.com). The eCognition approach to image segmentation is one of region merging whereby criteria are set that evaluate if two adjacent image objects are 'similar' based on their spectral and shape heterogeneity (Benz et al. 2004). The benefit of GEOBIA is that a defined set of steps can be established and applied in an automated procedure (Johansen et al. 2010). This represents a change in traditional image processing techniques which generally use purely statistically driven pixel-based approaches, often to good effect on moderate and low spatial resolution sensors. However, when applied to high spatial resolution images, like WV2, pixel-based approaches can produce mixed noisy results (Bernardini et al. 2010). The GEOBIA approach we have undertaken takes the atmospherically corrected image, masked for any trees above 2m (using canopy tree height layers derived from the LiDAR data), then creates a nested series of segmentations. The pre-processed images were processed to group pixels into segments that define the macrophytes as polygons. Each polygon or object, has been assessed as spectrally, texturally or contextually distinct. This distinction may be a function of species, object shape or morphology, and are derived using both spectral and spatial information. This results in a series of homogeneous objects which are then presented to a classifier.

The segmentation method was based on Baatz & Schape (2000) multi-resolution algorithm. Combinations of the scale, colour and shape parameters were assessed for each image analysed in a multi-step approach that produced image objects that retaining the overall homogeneous resolution of the image components. The scale defines the resolution of the subsequent image objects whereas the colour and shape indices are weighting functions, ranging from 0 to 1.

5.2 Unsupervised classification of ALOS and WV2 images

The objects were run through a fuzzy c-means (FCM) classifier in the MIPs software (TNTMips Pro, 2013). FCM classification is an unsupervised method that clusters data by weighting the class membership so that there are degrees of membership. It uses rules of fuzzy logic, which recognize that class boundaries may be imprecise or gradational. The FCM method creates an initial set of prototype classes then determines a membership grade for each class for every cell (Alata et al., 2008). The grades are used to adjust the class assignments and calculate new class centres, and the process repeats until the iteration limit is reached (TNTMips Pro, 2013). FCM provides more detailed information and allows interpretation of the results and produces a more natural class appearance compared to other classification methods (Leguizamon et al. 1996). In all cases the FCM classifier was allowed to define fifty classes to improve class homogeneity which was iterated through 100 classification passes.

5.3 Elevation mask

A 2011 LiDAR acquisition of the Kakadu floodplains was made available to this project by ERISS (Dept Environment, SSD). The massive volume of point data collected from the Kakadu LiDAR Survey 2011 was processed by Fugro Spatial Solutions into rasters in ESRI Grid™ format. Each individual Grid contains 1000 x 1000 cells in rows and columns respectively. The cell size represents 1 x 1 metres so each Grid represents 1 square kilometre. There are 4941 Grids which form a tiled mosaic of the flood plains and estuaries of Kakadu National Park. These tiled mosaics were used to subset the floodplains and create layers of the following (see Appendix A.5):

- Digital elevation Model (DEM)
- Canopy height model (CHM)
- Forest canopy model (FCM)

The image data was masked based on the CHM into a tree image (defined as CHM>2m) and a sub-canopy image for further interpretation.

5.4 Inundation frequency mask

Using an inter-annual floodplain inundation extent product, (produced from Ward et al, 2014), the sub-canopy images were further separated based on inundation frequency. Inundation frequency can be used as a surrogate of long term patterns of inundation duration. The method developed by Ward et al. (2014) delineated broad floodplain cover states which were utilised to separate the broad ecological classes within the imagery. The Ward et al. 2014 results were then used to separate the regions in the satellite imagery for this study. A threshold of 7 years was used to define whether the area was subject to regular inundation (and therefore wet) or areas that were more regularly dry. The 'wet' and 'dry' portions were compared with the field data as described in Table 4 and labelled accordingly.

Table 4 Classification layer fields

Field	Description
Value	This field refers to the original, unlabeled 50 classes. These classes were derived from the GEOBIA segmentation product, using an unsupervised fuzzy C-means spectral clustering procedure.
Class/ Label	This field is our vegetation class label, based on ○ a spectral similarity dendrogram of the original 50 classes ○ expert knowledge ○ *in situ* data.
Inundation	This field has a value of 1 or 2, depending on the inundation frequency mask that was applied to each polygon. ○ 1: these areas have a high inundation frequency, associated with frequent/permanent fresh water inundation (classes 8-17 of the inundation frequency maps) ○ 2: these areas have low inundation frequency, associated with seasonally/infrequent fresh water inundation and higher salinity (classes 1-7 of the inundation frequency maps)

5.5 Interpretation

The segmentation approach produced a spatially cohesive result, and the derived classes were assessed based on the spatial and spectral co-occurrence statistics, using the FCM dendogram for each classified image (e.g. Figure 5) and through visual interpretation.

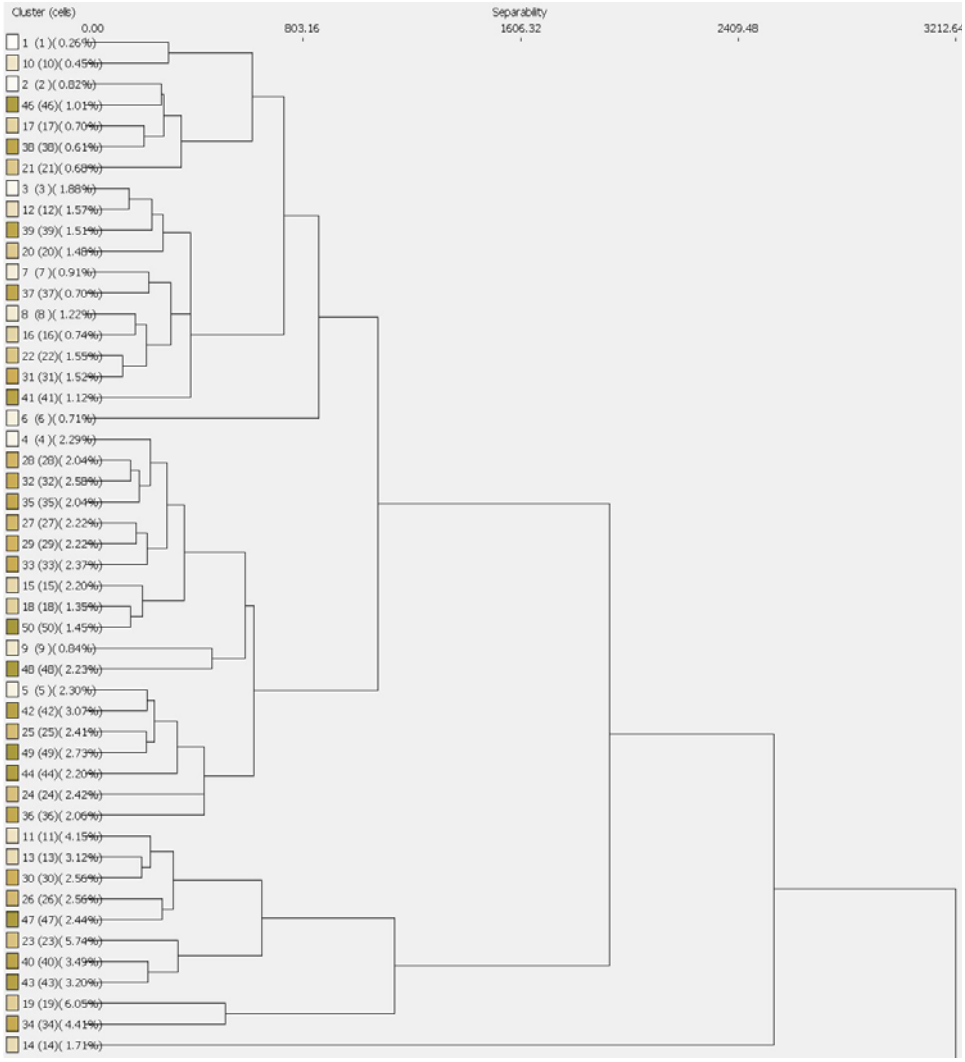

Figure 5 Example of a FCM dendrogram of the spatial and spectral co-occurrence statistics of the classification results of the 2012 Boggy Plains WV2 image. Above is the classification dendrogram (Euclidean clustering), that shows the degree of relatedness between the classes. Classes that are linked near the left edge of the dendrogram are more closely related whereas the degree of relatedness decreases further to the right.

The clustering of the classification floodplain vegetation groups in the dendrogram were compared with video transects of the South Alligator River floodplain, acquired by Charles Darwin University in June 2012 (Figure 6). A local expert (with sufficient time) was required to interpret the video data. This was done by James Boyden from the Environmental Research Institute of the Supervising Scientist (eriss), Department of Environment. Based on James Boyden's interpretation that identified species along transects, then clusters were assigned a species name. Where classes did not occur in areas along the Charles Darwin University helicopter transect sites, they were assigned a generic name. The rest of the helicopter data provided a validation source for the resultant classifications.

The Magela floodplain interpretation was aided by data collected from permanent vegetation plots which were periodically visited by CDU staff (Figure 6, Table 5).

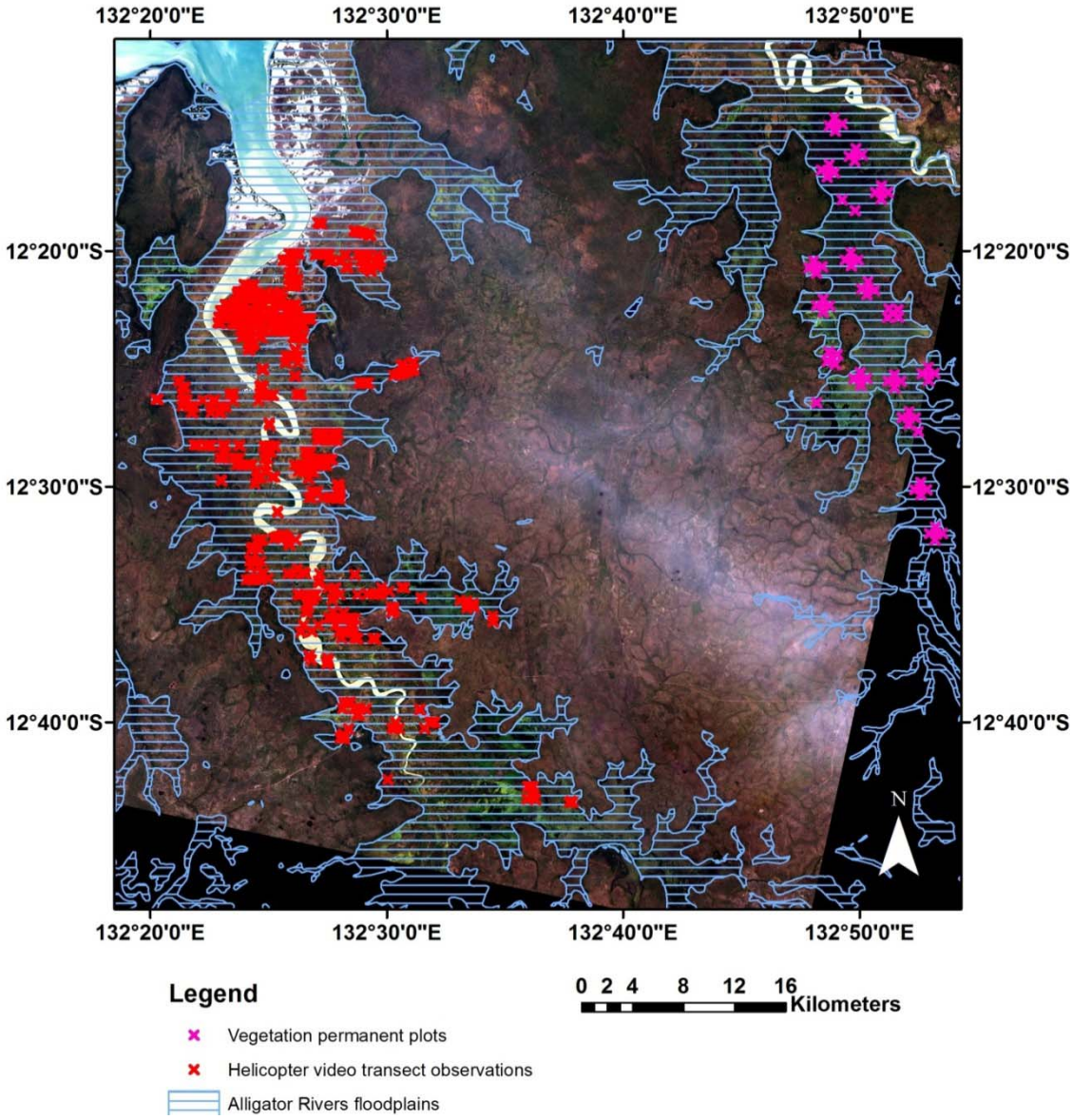

Figure 6 The ALOS AVNIR 13 May 2010 satellite image showing the locations of the Magela vegetation permanent plots and the 2012 South Alligator River interpreted helicopter video transect points.

The labelling was assisted (greatly) by local expert knowledge gained on our last trip to Darwin and Kakadu. We have attempted to incorporate this into the classification products we produced.

Validation data sources included:

- Past maps (Finlayson, Boyden et al, 2003, Whiteside and Bartolo, 2014)
- Peter Christophen and Sandra MacGregor (Kakadu Native Nursery)
- Buck Salau, Fred Baird & Ben Thornton (Kakadu National Park)
- CDU permanent vegetation plots (Magela)
- Helicopter video data (for sections of the South Alligator floodplain).

5.6 Accuracy Assessment

Classification accuracy was estimated using standard post-classification statistical analysis tools. Classified pixels were compared with ground-truth data, represented in this project by the Charles Darwin University (CDU) transect data and vegetation plots (Figure 6, Table 5). Classification accuracy was reported as the percentage of pixels classified correctly as well as the classes into which pixels that were incorrectly

classified were labelled. Cover types that are spectrally similar are more likely to be misclassified than spectrally unique classes.

Each of the CDU helicopter video transects or vegetation plots that intersected with the ALOS and WorldView-2 classifications were compared to produce an error matrix, or confusion matrix, for each region and date. Accuracy assessment was done only for data derived from the ALOS-AVNIR image of the Magela and South Alligator River regions and the Boggy Plains WV2 images. There was insufficient *in situ* data available for the West Alligator River, Yellow Waters and Munmalary areas of interest (AOIs). The available field data, although high quality for the purpose for when it was acquired, was not sufficient for accurate assessment of the satellite derived vegetation maps. Discrepancy in scale of the field data to the satellite data resulted in accuracy issues where the point measurement was spatially offset; this was obvious in highly heterogeneous areas where several different point measurements would be located within a single ALOS pixel. The solution for this was to intersect these point measurements with 30m polygon segments derived from the satellite data. The image-based segmentation was undertaken to delineate homogeneous features which could then be correlated spatially to the field observations. However, some of the 30m polygons were not spatially aligned with the correct pixels of the satellite image, leading to spatial heterogeneity.

Temporal discrepancies between the field acquired data and the satellite acquisition, meant that the currency of the field data was not always compatible, due to difference in dates and/or season. Therefore external knowledge or a priori information was utilised where appropriate and assisted in the labelling of the classification maps where no other information existed (see 5.5). It was also acknowledged that the dynamic nature of the vegetation and surface waters in some of the floodplain areas made them inappropriate for validation unless there was a reasonable match in dates.

As the dates of the field data and the satellite acquisitions were not exactly comparable (as shown in **Error! Reference source not found.**), there was over 36 months between the classification and the field validation dataset in the worst case and one week in the best case. This time offset must be taken into account when assessing the classification accuracy. More difficult to assess was the broad classes assigned to the helicopter video data. These broad classes were difficult to compare directly with the more detailed satellite derived classes which had been labelled on the basis of the a different set of helicopter transect data, previous remote sensing assessments and integrating expert knowledge from traditional owners and Parks staff (see acknowledgements). Attempts to collate the satellite classification classes in a similar manner to the helicopter data reduced the complexity and detail of the classes, particularly in the broader ALOS data.

Obvious misclassifications can be further assessed with more recent field observations, but areas where high accuracy was achieved could be utilised as surrogates that represent attributes that characterise the biodiversity for time series analyses.

Table 5 Dates of the satellite images and the transects used in their validation

Satellite image	Video transect date	Vegetation plot observation date	Time difference
13 May 2010 – ALOS (S. Alligator)	June 2012		25 Months
13 May 2010 – ALOS (Magela)		March 2009 May & June 2011 April & May 2012 May2013	-14 Months +12-13 Months +23-24 Months +36 Months
16 July 2010 – WV2	June 2012		+24 Months
6 June 2012 – WV2	June 2012		0 Months

6 Results and Discussion

6.1 GEOBIA results

Classification accuracy of the South Alligator River floodplain (Table 6), the Magela floodplain (Table 7) and Boggy Plains (Table 8 and Table 9) are presented in confusion matrix format. A confusion matrix is a row by column table where each row of the table represents the satellite-derived classes and each column displays the corresponding ground truth classes (from the Charles Darwin University transects/vegetation permanent plots) in the identical order. Overall accuracy is calculated by dividing the total number of pixels that were correctly classified, i.e. assigned to the correct class, by the total number of validation pixels or reference points used to construct the error matrix (Congalton 1991). Although the overall accuracy is the most commonly used accuracy measure, it does not take into account both errors of commission and omission for all individual classes.

The producer accuracy is the probability of a reference data point being classified correctly, whereas the user accuracy is the probability of a classified pixel being correct. The user and producer accuracies determine where misclassification has occurred, and where pixels have been erroneously excluded (omission), or included (commission), in an image class. The producer accuracy for a particular class is calculated for each column by dividing the number of correctly identified class pixels by the column total pixels. The user accuracy is calculated for a class by dividing the number of correctly identified class pixels by the row total pixels.

The kappa coefficient (varying between 0 and 1) reports the statistical measure of the extent to which the classification is a correct representation of the Charles Darwin University transect data. The kappa coefficient is a measure of the improvement by a classifier compared to a purely random assignment of classes. The higher the kappa coefficient value, the closer the agreement.

6.2 ALOS image classifications

The combined result of the ALOS 13 May 2010 classification is presented in Figure 7.

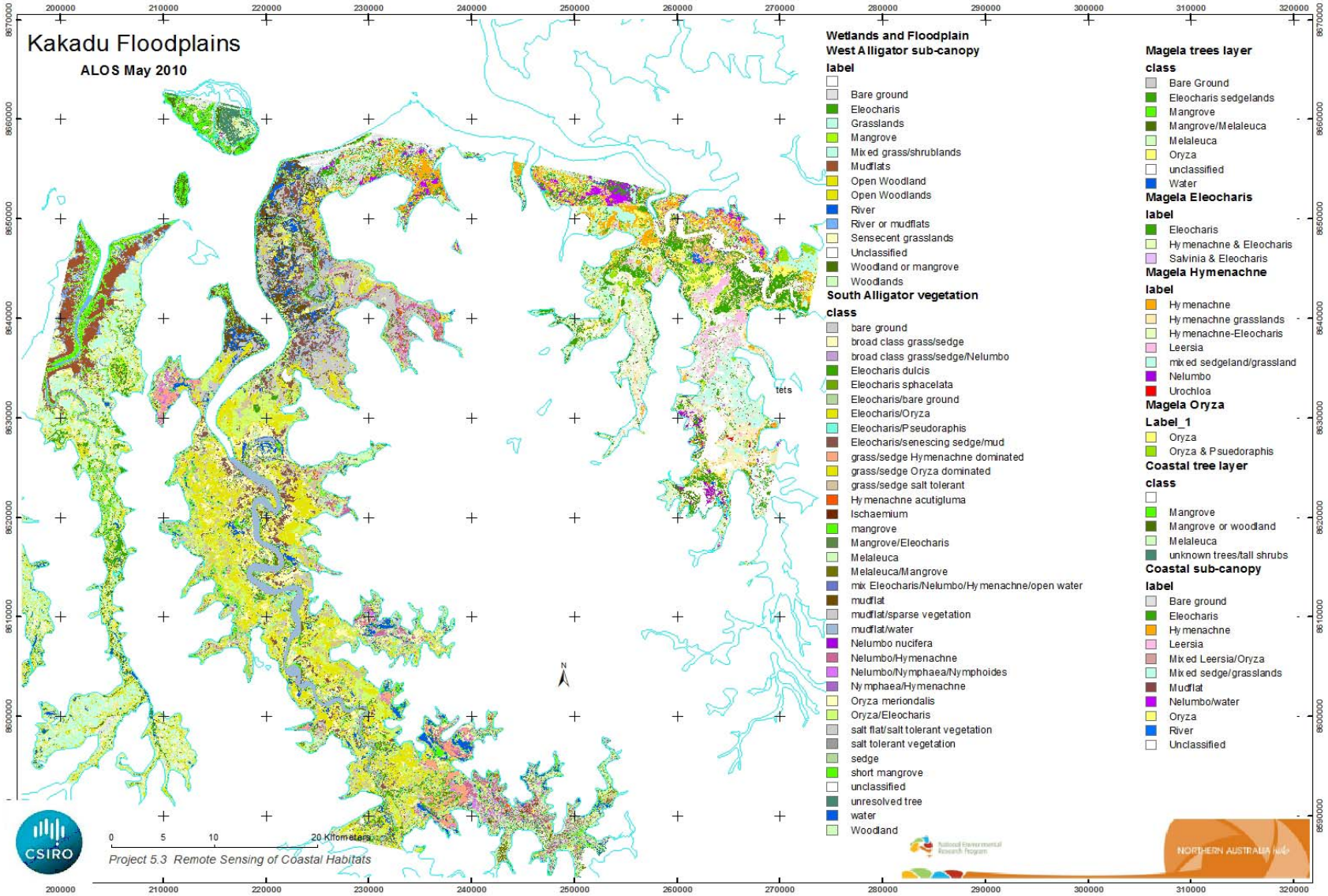

Figure 7 The Kakadu floodplain vegetation map for the 13th May 2010 ALOS image.

6.2.1 SOUTH ALLIGATOR ALOS CLASSIFICATION

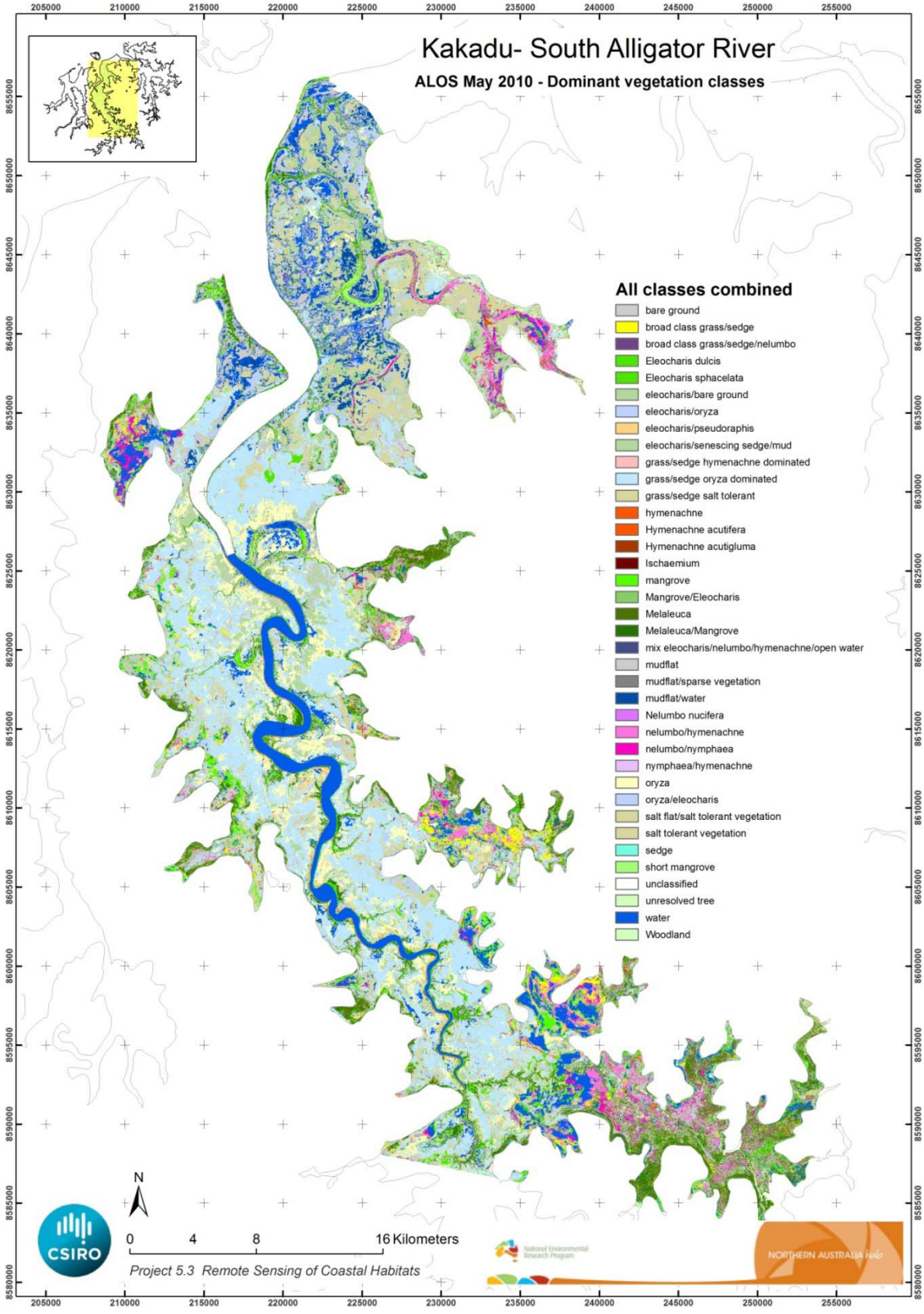

Figure 8 The South Alligator classification for 13 May 2010 ALOS image.

The South Alligator map (Figure 8) consists of two layers:

- **Sub-canopy**, frequently inundated (all the vegetation with a canopy height <2m, as determined from the LiDAR survey, which was inundated >7 years in the inundation frequency survey). This layer consists of four classes:
    - mangrove
    - broad class, consisting of *Eleocharis*/*Nelumbo*/*Hymenachne*
    - *Hymenachne* (sub-classes: pure *Hymenachne* (green or senescent), *Hymenachne* mixed with grass/sedge, *Hymenachne* mixed with *Nelumbo*)
    - *Nelumbo* (sub-classes: *Nelumbo* mixed with *Hymenachne*, *Nelumbo* mixed with nymphaea)

- **Sub-canopy**, dry/saline (all the vegetation with a canopy height <2m, as determined from the LiDAR survey, which was inundated <7 years in the inundation frequency survey). This layer consists of four major classes:
    - *Eleocharis* (sub-classes: *Eleocharis* Dulcis, *Eleocharis* mixed with *Oryza*, *Eleocharis* mixed with pseudoraphis)
    - *Oryza* (sub-classes: pure *Oryza*, *Oryza* mixed with pseudoraphis)
    - broad class grass/sedge (green and senescent)
    - salt flats/salt tolerant vegetation

Table 6 presents the classification accuracy of the South Alligator River floodplain vegetation map derived from the 13 May 2010 ALOS image. Validation data was obtained from the June 2012 helicopter video survey (Figure 6). There was a 25 month time difference as well as seasonal discrepancy between the satellite acquisition and the *in situ* observations. For this reason the classes were concatenated into broad vegetation groups to enable meaningful validation of the mapping results. For a detailed presentation of the accuracy assessment, please refer to Appendix A.

Although the overall accuracy of the simplified classification scheme is 64.3%, it is clear from Table 6 that not all groupings had a good correlation between the satellite-derived classes and the *in situ* observations. For example the freshwater *Nelumbo*/*Eleocharis*/grass/sedge grouping was predominantly miss-classified as water/ mudflats. This misclassification can be explained by the ephemeral nature of the location of *Nelumbo* and *Eleocharis* from year to year as well as seasonally. Due to the two year time lag between the satellite and *in situ* data, flooded areas that were covered in *Nelumbo*, mixed with *Eleocharis*, during one year may be open water in another year. The satellite image was also acquired at the end of the wet season while the helicopter video data was collected at the beginning of the dry season. This could have resulted in the extent and abundance of vegetation that thrives in flooded areas to be different in the two datasets. Vegetation that are located in areas that are more frequently dry as well as salt tolerant vegetation will have a more permanent presence, as can be observed in the more accurate classification of the *Oryza*/salt tolerant grouping.

Table 6 The classification accuracy result for ALOS South Alligator Rive floodplain where each row of the table represents the satellite-derived classes and each column displays the corresponding ground truth classes (from the helicopter video survey) in the identical order. Overall classification accuracy is 64.3%.

percentage %	*Nelumbo/Eleocharis*/grass/sedge senescing	*Oryza* / Salt tolerant vegetation	trees	water or mudflats	row total	user accuracy
***Nelumbo*/*Eleocharis*/grass/sedge senescing**	**1.1**	2.2	1.3	0.5	5.1	22.2%
***Oryza*/salt tolerant vegetation**	4.8	**92.3**	9.8	8.3	115.2	80.1%
trees	0.1	0.8	**15.6**	0.1	16.6	93.8%
water or mudflats	93.9	4.7	73.4	**91.1**	263.1	34.6%
column total	100.0	100.0	100.0	100.0		
producers accuracy	1.1%	92.3%	15.6%	91.1%		
kappa	0.4442	0.3490	0.4447	0.3970		
tau	0.4278	0.3265	0.4278	0.3241		

6.2.2 MAGELA ALOS CLASSIFICATION

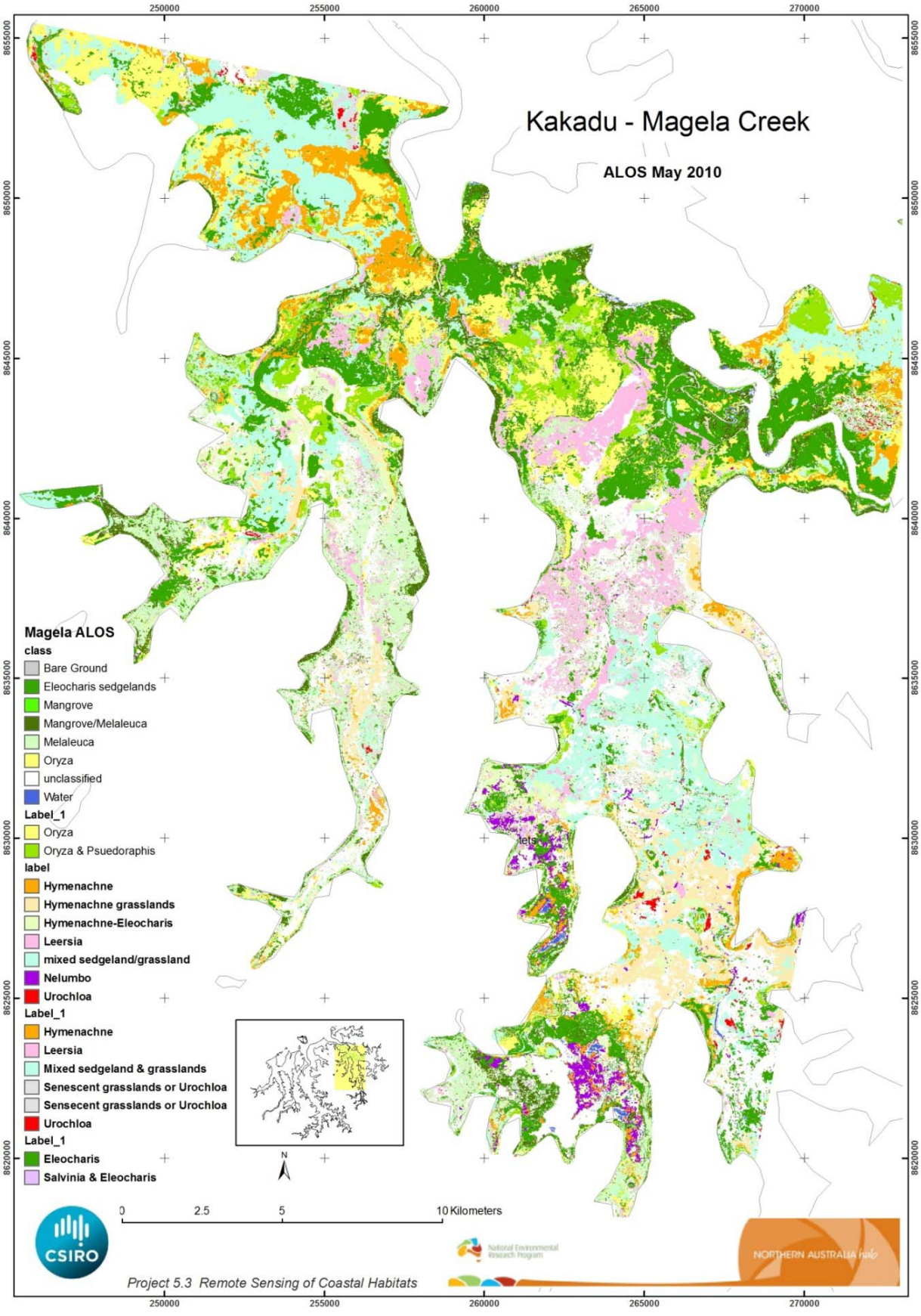

Figure 9 The Magela classification for 13 May 2010 ALOS image.

The Magela ALOS map (Figure 9) consists of two layers:

- Sub-canopy, frequently inundated (all the vegetation with a canopy height <2m, as determined from the LiDAR survey, which was inundated >7 years in the inundation frequency survey). This layer consists of seven major classes:

    - *Eleocharis* (sub-classes: pure *Eleocharis*, *Eleocharis* mixed with *Salivinia*)
    - *Hymenachne* (sub-classes: pure *Hymenachne* (green or senescent), *Hymenachne* mixed with grass/sedge)
    - *Oryza* (sub-classes: pure *Oryza*, *Oryza* mixed with *Pseudoraphis*)
    - *Nelumbo*
    - broad class grass/sedge
    - *Leersia*
    - *Urochloa*

- Sub-canopy, dry/saline (all the vegetation with a canopy height <2m, as determined from the LiDAR survey, which was inundated <7 years in the inundation frequency survey). This layer consists of six major classes:

    - *Eleocharis* (sub-classes: pure *Eleocharis*, *Eleocharis* mixed with *Salivinia*)
    - *Hymenachne*
    - *Oryza* (sub-classes: pure *Oryza*, *Oryza* mixed with *Pseudoraphis*)
    - broad class grass/sedge (green and senescent)
    - *Leersia*
    - *Urochloa*

Table 7 presents the classification accuracy of the Magela floodplain vegetation map derived from the 13 May 2010 ALOS AVNIR image. Validation data was obtained from the April/May 2012 survey of the Magela permanent vegetation plots (Figure 6). There was a significant time difference between the satellite acquisition and the *in situ* observations (Table 5). For this reason the classes were concatenated into broad vegetation groups to enable meaningful validation of the mapping results. For a detailed presentation of the accuracy assessment, please refer to Appendix A.2.

The currency of field data is significantly reduced when acquired at a different season or with a significant time lag from the satellite image. This may account for the low overall accuracy of the Magela classification, as it was assessed using data from different seasons and with a time difference of up to 36 months (Table 5).

Vegetation occurring in areas that were flooded with fresh water at the time of the satellite acquisition, such as *Hymenachne* and *Nelumbo* were frequently misclassified. This misclassification can be explained by the ephemeral nature of the location of these vegetation types from year to year as well as seasonally. Due to the two year time lag between the satellite and *in situ* data, flooded areas that were covered in *Nelumbo*, mixed with *Hymenachne*, during one year may be open water in another year. Vegetation types also transition seasonally depending on rainfall and as the floodplains dry out. This may explain the frequent misclassifications of vegetation types that are spectrally similar (e.g. *Eleocharis*, *Hymenachne*, *Pseudoraphis* and *Oryza*).

Table 7 The classification accuracy result for ALOS Magela floodplain where each row of the table represents the satellite-derived classes and each column displays the corresponding ground truth classes (from the Magela permanent vegetation plot data) in the identical order. Overall classification accuracy is 26.7%.

percentage %	*Eleocharis*	*Hymenachne*	*Leersia*	mixed sedgelands and grasslands	*Nelumbo*	*Oryza*	*Oryza & Psuedoraphis*	Salvinia/*Eleocharis*	row total	user accuracy
Eleocharis	**37.0**	22.6	5.5	11.3	58.8	8.0	49.5	0.0	192.6	
Hymenachne	0.0	**0.0**	9.7	27.6	0.0	0.7	0.0	0.0	38.0	
Leersia	0.0	18.0	**35.6**	11.8	0.0	4.8	28.6	0.0	98.9	19.2%
Mixed sedgelands and grasslands	4.3	6.0	23.2	**24.1**	35.3	45.7	0.0	0.0	138.5	0.0%
Nelumbo	0.0	0.0	0.0	2.9	**2.0**	0.0	0.0	0.0	4.8	36.0%
Oryza	10.7	53.4	9.7	13.6	3.9	**33.9**	7.3	0.0	132.5	17.4%
Oryza* & *Psuedoraphis	48.0	0.0	16.4	8.6	0.0	6.9	**14.7**	0.0	94.7	40.6%
Salvinia/Eleocharis	0.0	0.0	0.0	0.0	0.0	0.0	0.0	**100.0**	100.0	25.6%
column total	100.0	100.0	100.0	100.0	100.0	100.0	100.0	100.0		
producers accuracy	37.0%	0.0%	35.6%	24.1%	2.0%	0.0%	14.7%	100.0%		
Kappa	0.2253	0.2302	0.2166	0.2176	0.2302	0.2255	0.2284	0.2302		
Tau	0.2222	0.2302	0.2171	0.2199	0.2301	0.2227	0.2272	0.2285		

6.2.3 WEST ALLIGATOR ALOS CLASSIFICATION

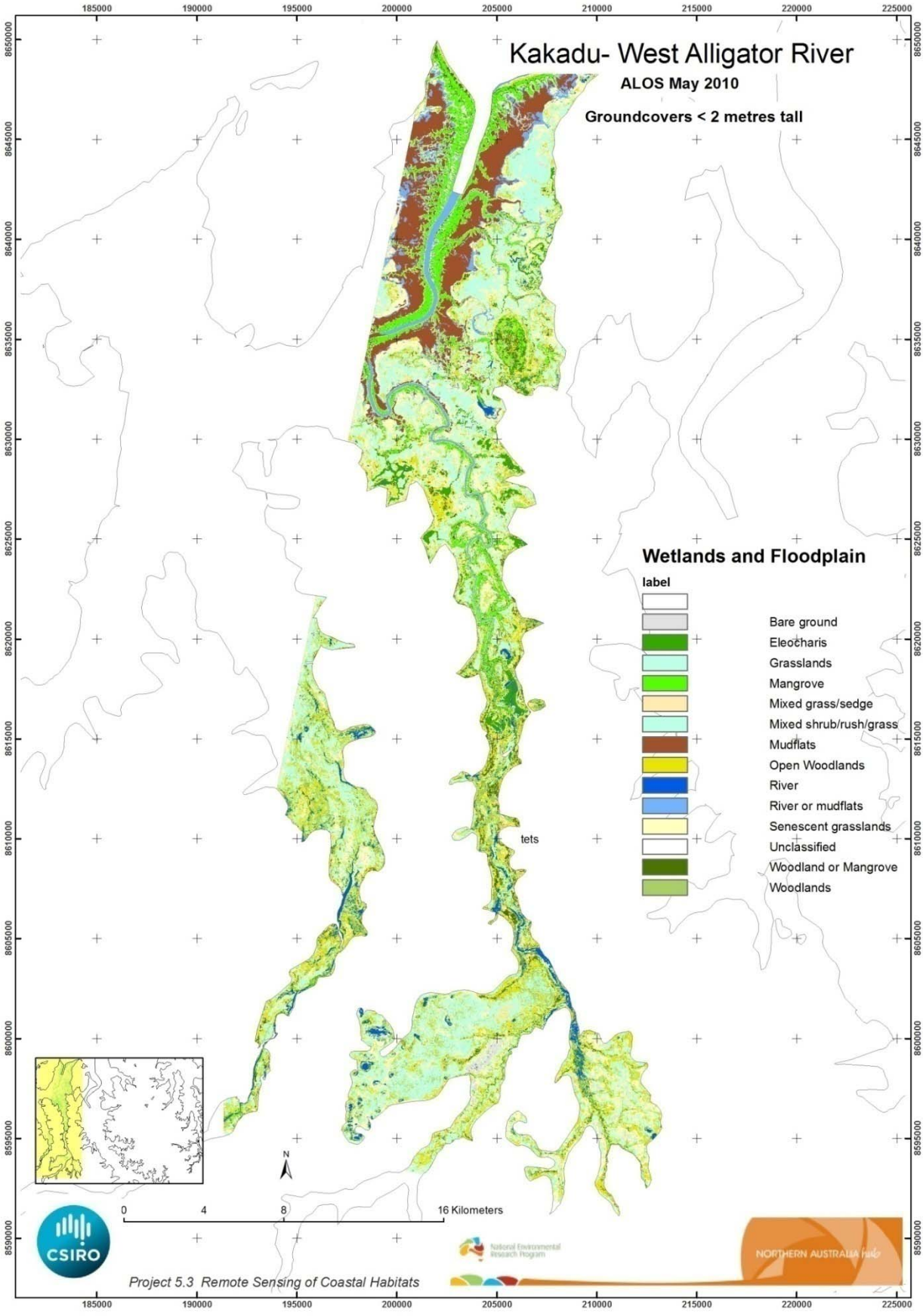

Figure 10 The West Alligator classification for 13 May 2010 ALOS image.

The West Alligator map (Figure 10) consists of one layer with 8 major classes:

- mangrove
- open woodland
- spectrally unresolved woodland (*Melaleuca*/mangrove)
- *Eleocharis*
- broad class of mixed grass/sedge
- broad class senescent grass/sedge
- bare soil/mud/sparse vegetation
- water

For this region we were unable to acquire sufficient validation data to undertake an accuracy assessment. Classification labelling was based on input from local experts (see 5.5) viewing the imagery and corresponding spectral classes in the South Alligator classification.

6.2.4 COASTAL ALOS CLASSIFICATION

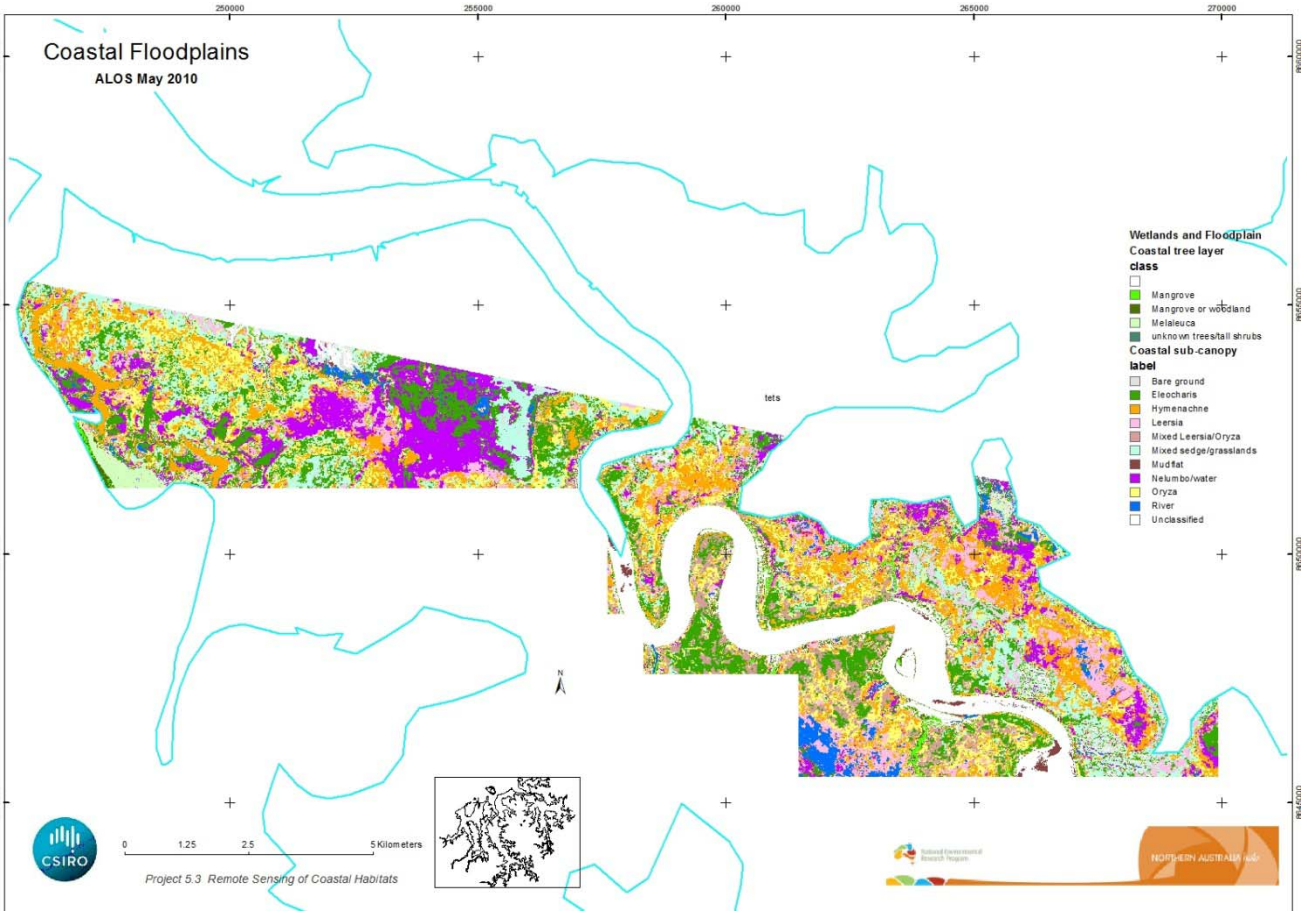

Figure 11 The coastal floodplain classification for 13 May 2010 ALOS image.

The coastal floodplain map (Figure 11) consists of two layers:

- **Canopy** (all the vegetation with a canopy height >2m, as determined from the LiDAR survey). This layer consists of four major classes:
    - mangrove
    - *Melaleuca* woodland
    - spectrally unresolved woodland (*Melaleuca* /mangrove)
    - woodland (located in dry floodplain areas)
- **Sub-canopy** (all the vegetation with a canopy height <2m, as determined from the LiDAR survey). This layer consists of eight major classes:
    - *Eleocharis*
    - *Hymenachne*
    - *Leersia* (sub-class: pure *Leersia*, *Leersia* mixed with *Oryza*)
    - *Oryza* (sub-class: pure *Oryza*, *Leersia* mixed with *Oryza*)
    - broad class of mixed grass/sedge
    - *Nelumbo*
    - bare soil/mud/sparse vegetation
    - water

For this region we were unable to acquire sufficient validation data to undertake an accuracy assessment. Classification labelling was based on input from local experts (see 5.5) viewing the imagery and corresponding spectral classes in the Magela classification.

6.2.5 MUNMARLARY WV2 IMAGE CLASSIFICATION

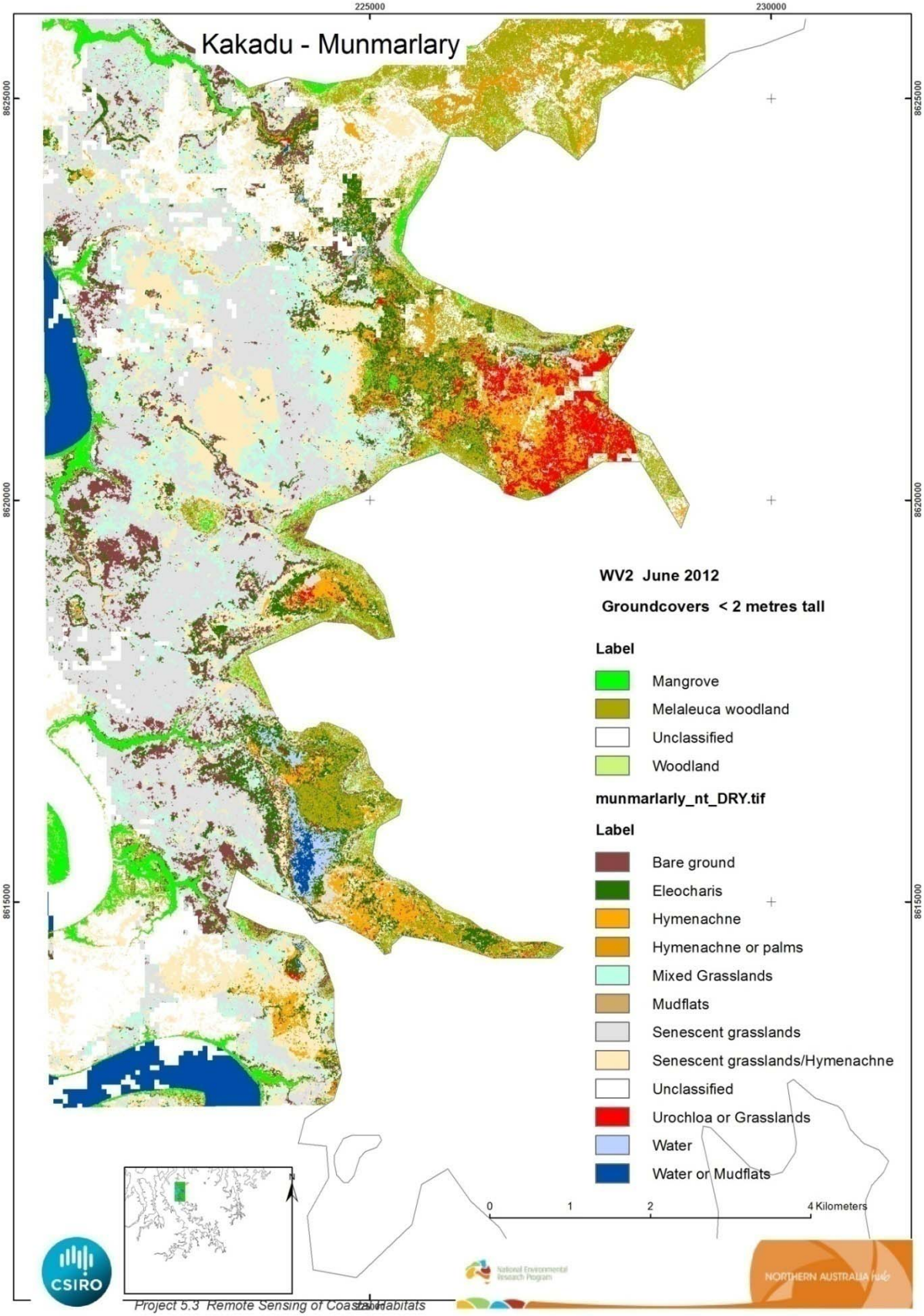

Figure 12 The Munmarlary floodplain WV2 classification for 6 June 2010.

The Munmarlary map (Figure 12) consists of two layers:

- **Canopy** (all the vegetation with a canopy height >2m, as determined from the LiDAR survey. This layer consists of three major classes:
    - mangrove
    - *Melaleuca* woodland
    - woodland (located in dry floodplain areas)
- **Sub-canopy**, dry/saline (all the vegetation with a canopy height <2m, as determined from the LiDAR survey, which was inundated <7 years in the inundation frequency survey). This layer consists of six major classes:
    - *Eleocharis*
    - *Hymenachne*
    - (sub-class: pure *Hymenachne*, *Hymenachne* mixed with grass/sedge, *Hymenachne* that may be spectrally confused with palms)
    - broad class of senescent grass/sedge
    - *Urochloa*/grasslands

For this region we were unable to acquire sufficient validation data to undertake an accuracy assessment. Classification labelling was based on input from local experts (see 5.5) viewing the imagery and corresponding spectral classes in the South Alligator classification.

6.2.6 BOGGY PLAINS WV2 IMAGE CLASSIFICATIONS

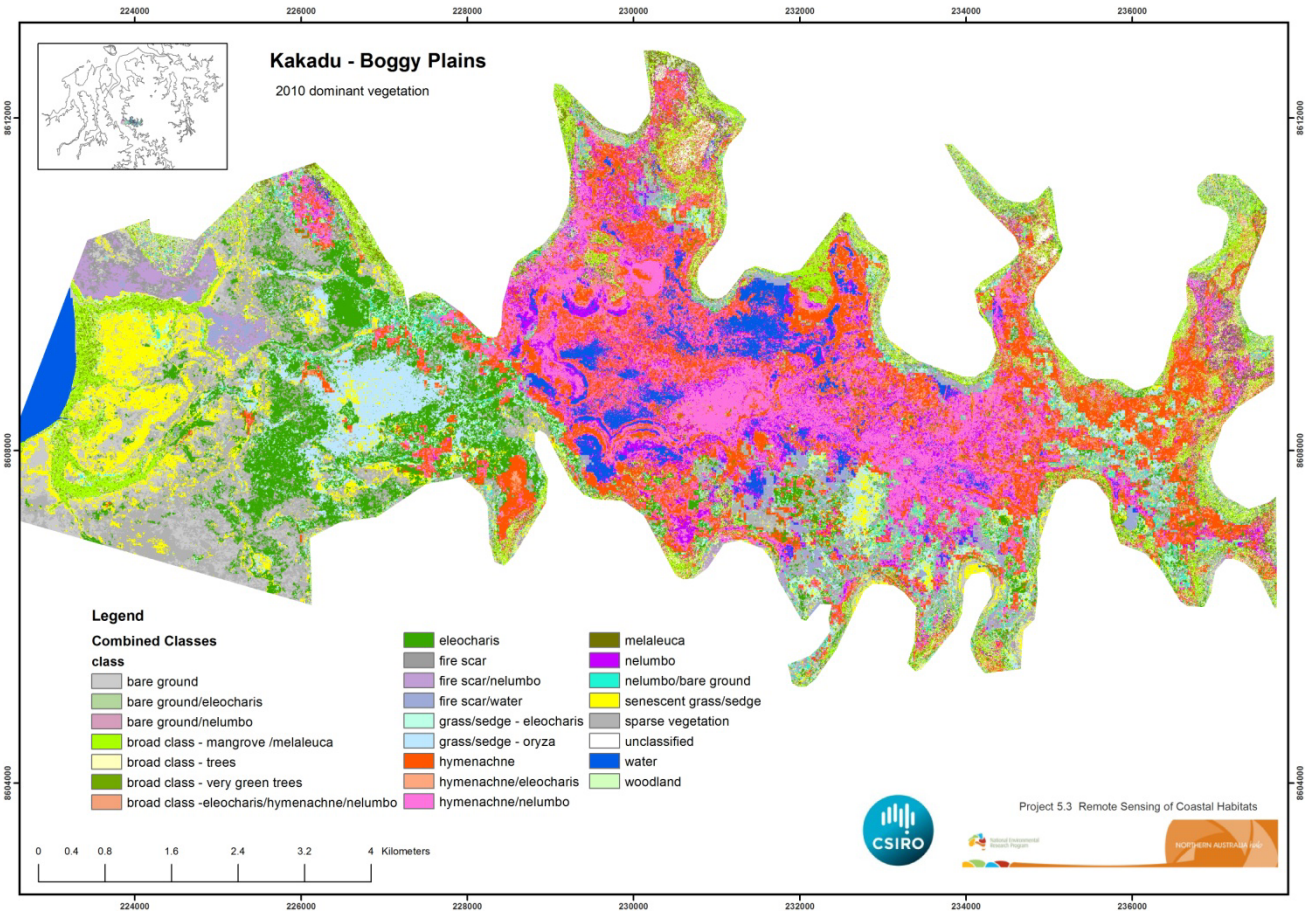

Figure 13 The Boggy Plains floodplain WV2 classification for 6 June 2010.

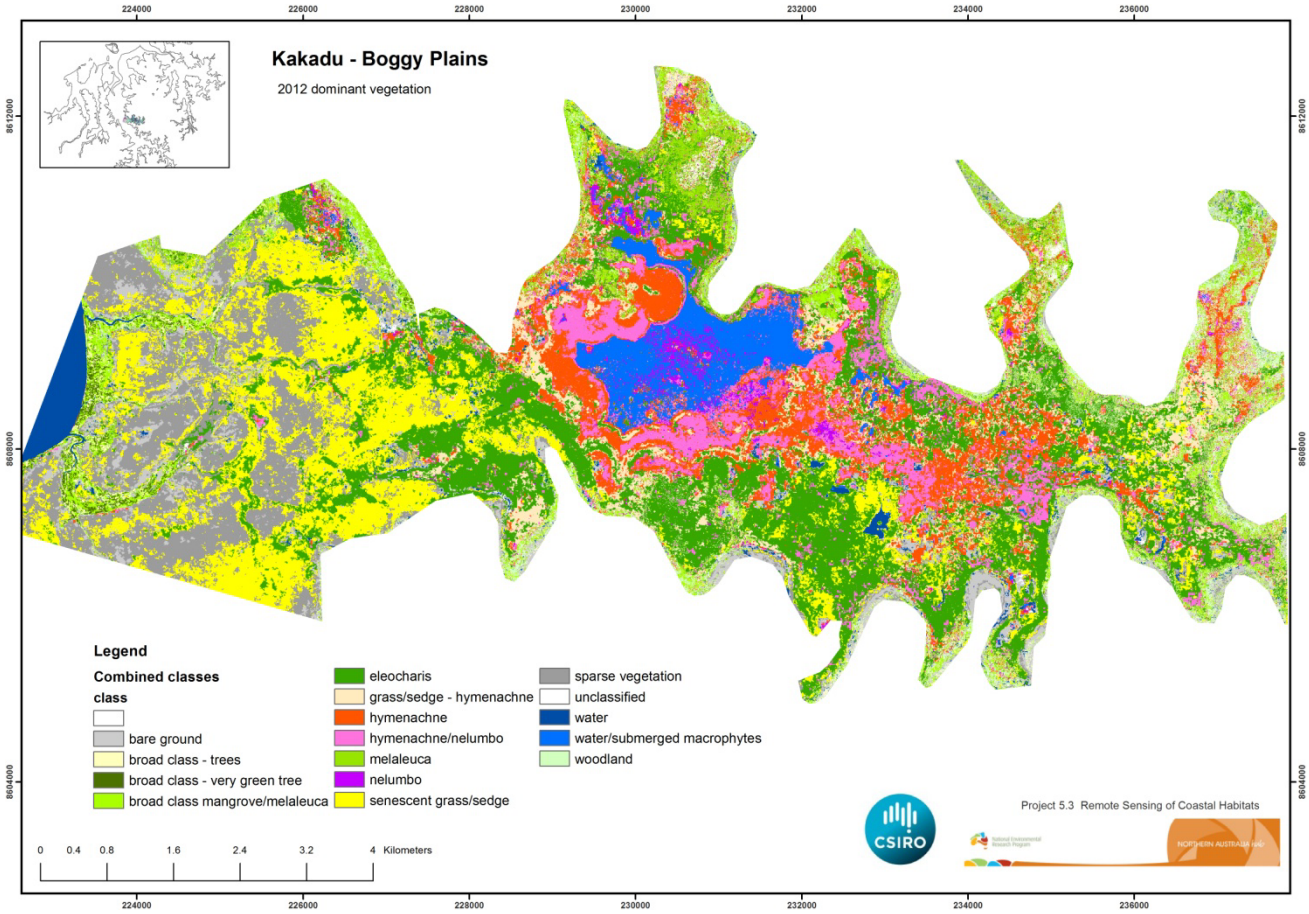

Figure 14 The Boggy Plains floodplain WV2 classification for 16 July 2012.

These maps (Figure 13-14) consist of two layers:

- **Sub-canopy**, frequently inundated (all the vegetation with a canopy height <2m, as determined from the LiDAR survey, which was inundated >7 years in the inundation frequency survey). This layer consists of seven major classes:
    - *Eleocharis* (sub-classes: pure *Eleocharis*, *Eleocharis* mixed with *Hymenachne*)
    - *Hymenachne* (sub-classes: pure *Hymenachne* (green or senescent), *Hymenachne* mixed with grass/sedge, *Hymenachne* mixed with *Nelumbo*, *Hymenachne* mixed with *Eleocharis*)
    - *Nelumbo* (sub-classes: pure *Nelumbo*, *Nelumbo* mixed with *Hymenachne*)
    - broad class, consisting of *Nelumbo/ Hymenachne /Eleocharis*
    - broad class of senescent grass/sedge
    - bare soil/mud/sparse vegetation
    - water
- **Sub-canopy**, dry/saline (all the vegetation with a canopy height <2m, as determined from the LiDAR survey, which was inundated <7 years in the inundation frequency survey). This layer consists of six major classes:
    - *Eleocharis* (sub-classes: pure *Eleocharis*, *Eleocharis* mixed with grass/sedge)
    - *Hymenachne*
    - *Oryza* mixed with grass/sedge
    - broad class of senescent grass/sedge
    - bare soil/mud/sparse vegetation/fire scar
    - water

Table 8 presents the classification accuracy of the Boggy Plains region of the South Alligator River floodplain vegetation map derived from the 16 July 2010 WV2 image. Validation data was obtained from the June 2012 helicopter video survey (Figure 6). There was a 24 month time difference between the satellite acquisition and the *in situ* observations. For this reason the classes were concatenated into broad vegetation groups to enable meaningful validation of the mapping results. For a detailed presentation of the accuracy assessment, please refer to Appendix A.3.

The overall accuracy of the simplified classification scheme is 87.5%. A notable exception to the good overall correlation between the satellite derived classes and the *in situ* observations is the low classification accuracy of the *Nelumbo* class. This class was classified as *Hymenachne* in the 2010 ALOS satellite image. This apparent misclassification can be explained by the ephemeral nature of the location of *Nelumbo* and *Hymenachne* from year to year. Due to the two year time lag between the satellite and *in situ* data, flooded areas that were covered in *Nelumbo* may be covered in *Hymenachne* or a mix of *Nelumbo* and *Hymenachne* in another year.

Table 8 The classification accuracy result for the 2010 WV2 Boggy Plains floodplain where each row of the table represents the satellite-derived classes and each column displays the corresponding ground truth classes (from the helicopter video survey) in the identical order. Overall classification accuracy is 87.5%.

percentage %	*Eleocharis*	*Hymenachne*	grass/sedge - *Oryza*	*Nelumbo*	senescent grass/sedge	water	row total	User accuracy
Eleocharis	**0**	0.0	0.0	0.0	0.0	0.0	0.0	0.0
Hymenachne	0	**90.8**	31.0	98.9	0.0	0.0	220.7	60.5
grass/sedge – *Oryza*		7.7	**67.2**	0.0	14.7	0.0	89.6	39.8
Nelumbo	0	0.2	0.1	**0.0**	0.2	0.0	0.50	0.0
senescent grass/sedge	0	1.2	1.7	0.0	**85.1**	0.0	88.0	99.3
Water	0	0.0	0.0	1.1	0.0	**99.9**	**101.0**	99.8
column total	0	100	100	100	100	100		
producers accuracy	0.0%	90.8%	31.0%	0.0%	85.1%	99.9%		
Kappa	0.0000	0.8742	0.8749	0.8749	0.8753	0.8574		
Tau	0.0000	0.8737	0.8747	0.8747	0.8753	0.8602		

Table 9 presents the classification accuracy of the Boggy Plains region of the South Alligator River floodplain vegetation map derived from the 6 June 2012 WV2 image. Validation data was obtained from the June 2012 helicopter video survey (Figure 6). Classes were concatenated into broad vegetation groups to enable meaningful validation of the mapping results. For a detailed presentation of the accuracy assessment, please refer to Appendix A.4.

The overall accuracy of the simplified classification scheme is 88.5%. An exception to the good overall correlation between the satellite derived classes and the *in situ* observations is the low classification accuracy of the *Hymenachne* class which was frequently misclassified as *Eleocharis*. This could be explained by the spectral similarity of these two vegetation classes and the fact that *Eleocharis* frequently replaces

Hymenachne as the floodplains dry out at the end of the wet season. Both these factors could have resulted in labelling errors. *Nelumbo* and *Hymenache* frequently co-occur in the Boggy Plains region. This may explain the apparent misclassification of *Nelumbo* as *Hymenachne*.

Table 9 The classification accuracy result for the 2012 WV2 Boggy Plains floodplain where each row of the table represents the satellite-derived classes and each column displays the corresponding ground truth classes (from the helicopter video survey) in the identical order. Overall classification accuracy is 88.5%.

percentage %	*Eleocharis*	*Hymenachne*	*Nelumbo*	senescent grass/sedge	water	row total	User accuracy
Eleocharis	**0**	79.5	0.0	0.0	0.0	79.5	0.0%
Hymenachne	0	**13.7**	56.9	4.3	0.0	74.9	18.3%
Nelumbo	0	5.8	**43.1**	0.0	0.1	49.0	88.0%
senescent grass/sedge	0	1.0	0.0	**95.4**	0.0	96.4	99.0%
water	0	0.1	0.0	0.3	**99.9**	100.3	99.6%
column total	0	100	100	100	100		
producers accuracy	0.0%	13.7%	43.1%	95.4%	99.9%		
kappa	0.8856	0.8855	0.8856	0.7742	0.8815		
tau	0.8856	0.8855	0.8856	0.7837	0.8814		

6.2.7 YELLOW WATERS WV2 IMAGE CLASSIFICATIONS

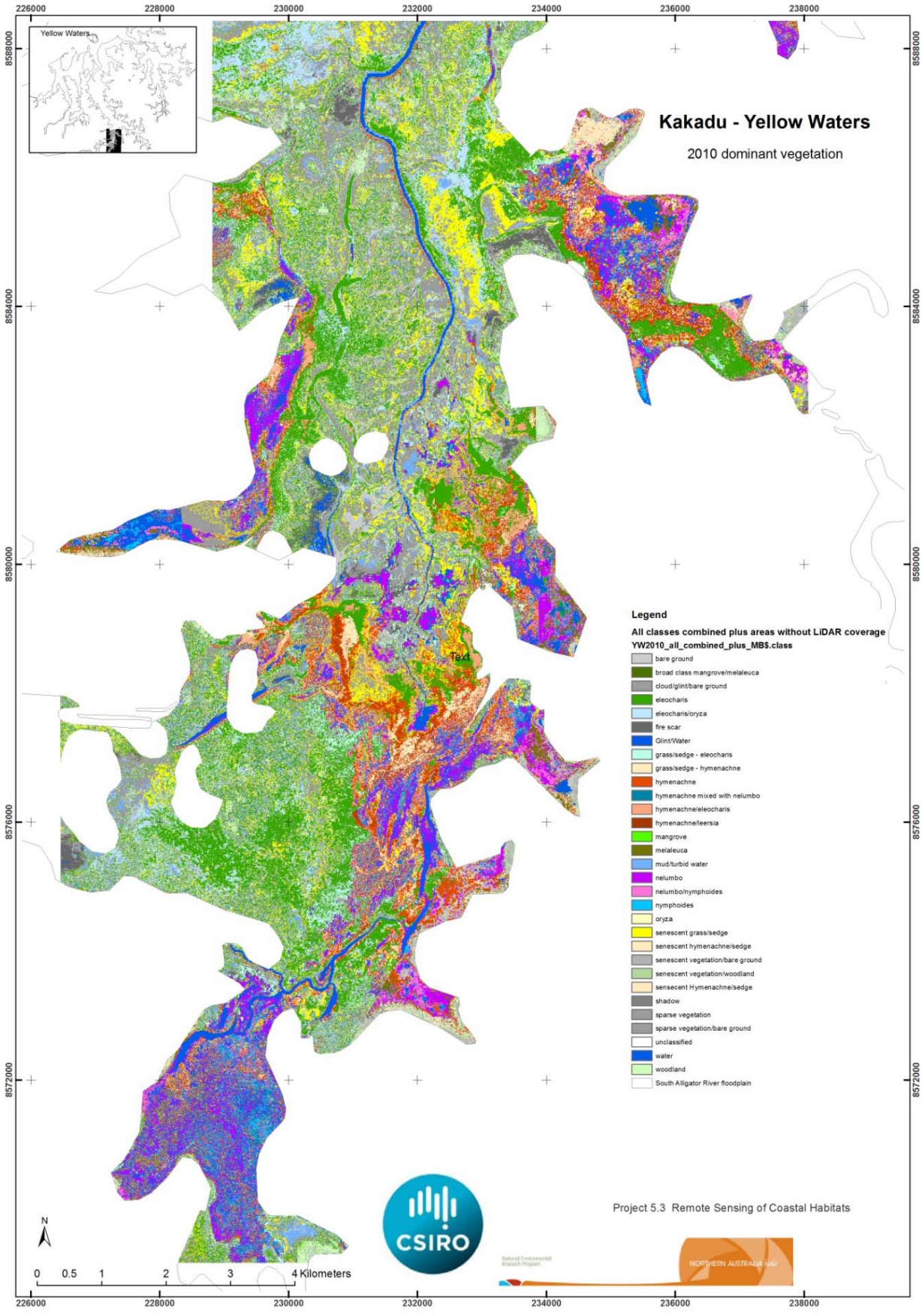

Figure 15 The Yellow Waters floodplain WV2 classification for 6 June 2010.

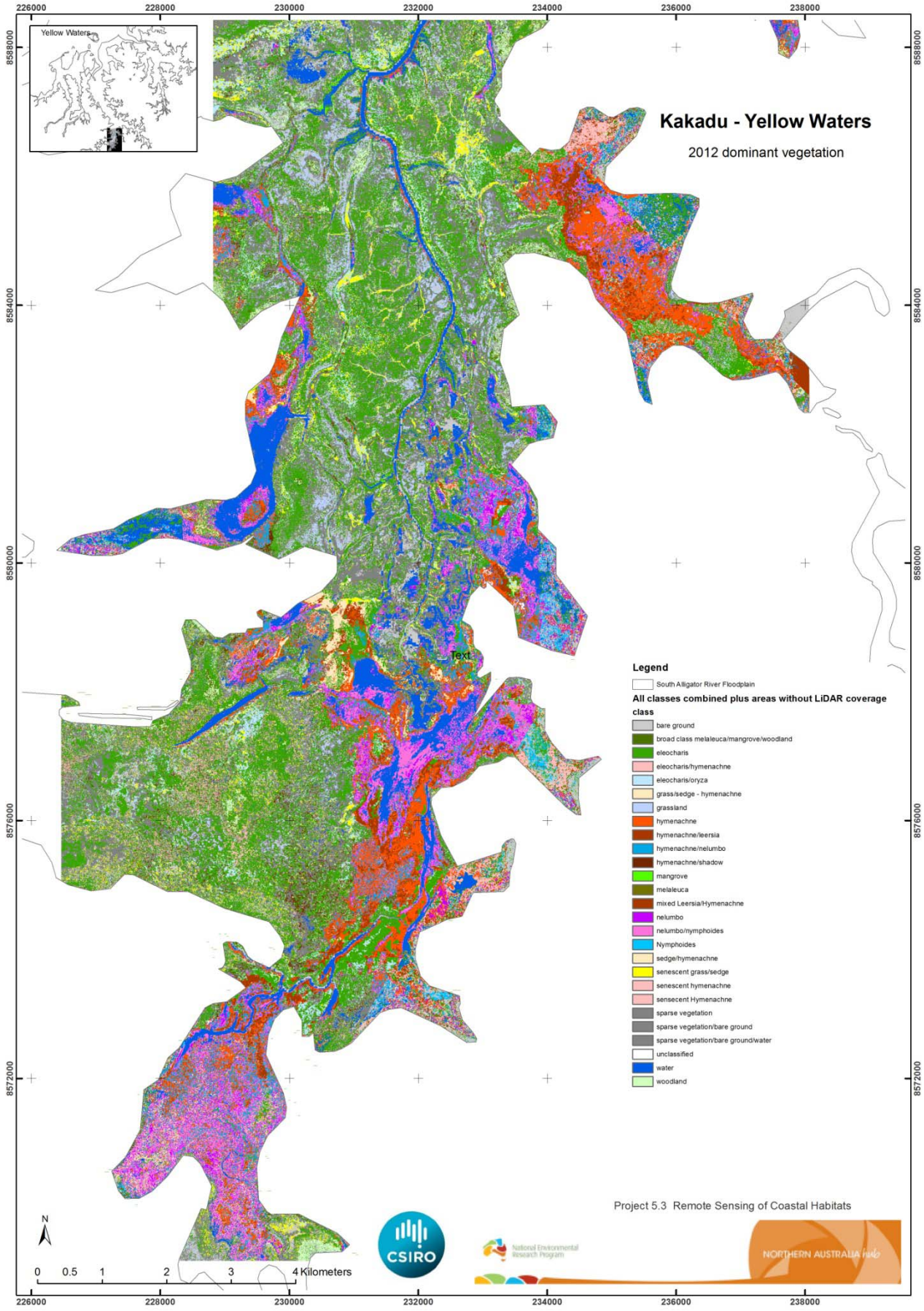

Figure 16 The Yellow Waters floodplain WV2 classification for 16 July 2012.

The Yellow Waters WV2 maps (Figure 15-16) consist of three layers:

- **Canopy** (all the vegetation with a canopy height >2m, as determined from the LiDAR survey. This layer consists of four major classes:
    - mangrove
    - *Melaleuca* woodland
    - woodland (located in dry floodplain areas)
    - spectrally unresolved woodland (*Melaleuca*/mangrove)
- **Sub-canopy**, frequently inundated (all the vegetation with a canopy height <2m, as determined from the LiDAR survey, which was inundated >7 years in the inundation frequency survey). This layer consists of six major classes:
    - *Eleocharis* (sub-classes: *Eleocharis*, *Eleocharis* mixed with *Hymenachne*)
    - *Hymenachne* (sub-classes: pure *Hymenachne* (green or senescent), *Hymenachne* mixed with grass/sedge, *Hymenachne* mixed with *Nelumbo*, *Hymenachne* mixed with *Eleocharis*, *Hymenachne* mixed with *Leersia*)
    - *Nelumbo* (sub-classes: pure *Nelumbo*, *Nelumbo* mixed with *Hymenachne*, *Nelumbo* mixed with nymphaea)
    - broad class of senescent grass/sedge
    - bare soil/mud/sparse vegetation
    - water
- **Sub-canopy**, dry/saline (all the vegetation with a canopy height <2m, as determined from the LiDAR survey, which was inundated <7 years in the inundation frequency survey). This layer consists of six major classes:
    - *Eleocharis* (sub-classes: pure *Eleocharis*, *Eleocharis* mixed with *Oryza*, *Eleocharis* mixed with grass/sedge)
    - *Hymenachne*
    - *Oryza*
    - broad class of senescent grass/sedge
    - bare soil/mud/sparse vegetation/fire scar
    - water

For the Yellow Waters region we were unable to acquire sufficient validation data to undertake an accuracy assessment. Classification labelling was based on input from local experts (see 5.5) viewing the imagery and corresponding spectral classes in the South Alligator classification.

6.3 Key Findings

1. The WorldView-2 data is sufficient to support detailed and accurate floodplain vegetation monitoring when of adequate quality.

2. The GEOBIA approach of weighted band segmentation and spectral difference aggregation developed a refined information-rich image base for input in a FuzzyC classification. This result better delineated the vegetation beds and produced less speckled classification results compared to traditional per-pixel based classification methods.

3. The classified images were separated based on an inter-annual floodplain inundation extent (Ward et al, 2014). Inundation frequency can be used as a surrogate of long-term patterns of inundation duration and enabled the identification of 'wet' and 'dry' floodplain vegetation types.

4. Accuracy assessment of the floodplain vegetation classifications was difficult to achieve with the available *in situ* and helicopter transect data. When the broad classes of the helicopter transect was compared to the satellite classification, it showed general agreement, despite the time and seasonal differences between the transects or vegetation plots and the image acquisition. The average overall accuracy when species classes were combined into one general floodplain vegetation class was 64.3% and 26.5% respectively, for the ALOS South Alligator and Magela images, which could be related to the dynamic nature of the Magela vegetation and surface waters. A better overall result was obtained for the 2010 and 2012 Boggy Plain WorldView2 imagery of 87.5% and 88.5% respectively.

7 Conclusions and Recommendations

Assessing the spatial distribution of floodplain environments using high resolution satellite imagery provides key information on the current condition, vulnerabilities and major causal factors of stresses upon the environment. An essential requirement for systematic environmental management using high spatial resolution satellites is for objective, repeatable processing pathways, eliminating operator bias and quantifying uncertainty.

High spatial resolution satellite imaging, especially with the increased number of spectral bands of WorldView2 enables significantly improved accuracy in floodplain vegetation classification and change detection analyses suitable for use in environmental management.

The resultant ALOS and WorldView2 floodplain vegetation maps produced provide a spatially dense picture of floodplain vegetation coverage in floodplains of the Kakadu NP. The floodplain vegetation assessment used advanced high spectral resolution techniques (such as atmospheric correction, field spectroradiometry and classification) consistently applied to the satellite imagery, in a repeatable, objective pathway developed for this project.

This approach for implementing high spatial resolution earth observation-derived habitat relevant data enables environmental base-lining, allowing periodic trend and condition assessment. When undertaking this integrated approach in future work, the key activities would involve:

- Environmental baseline collection through acquiring a suitable coverage of high spatial resolution satellite data.
- Spectral library acquisition.
- Classification and change detection.
- Acquisition of validation *in situ* data of floodplain vegetation concurrent with image capture, to adequately capture the vegetation dynamics on the floodplains.
- Identification of invariant features to calibrate models and methods.
- Coincident (or as close as possible) field work for the purposes of classification assessment.

Acknowledgements

This project was co-funded by CSIRO Wealth from Oceans Flagship and by the Australian Government's National Environmental Research Program (NERP). Charles Darwin University provided their helicopter transect data and historical vegetation plots which formed an integral part of this project. Thanks are extended to Parks and the Kakadu Native Nursery, and in particular Buck Salau, Fred Baird and Ben Thornton (Parks), James Boyden, Renee Bartolo and Tim Whiteside (eriss), Samantha Setterfield and Aaron Petty (CDU), Peter Bayliss (CSIRO) and Peter Christophersen and Sandra McGregor (Kakadu Native Nursery) for their input to the labelling of the classification.

8 References

Alata, M., Molhim,M. and Ramini, A. (2008), Optimizing of Fuzzy C-Means Clustering Algorithm Using GA, World Academy of Science, Engineering and Technology, p.224-229.

Anstee, J.M. and Byrne,G.T. (2014), *Assessing the feasibility of applying remote sensing to macrophyte monitoring: Appended final report.* Water from a Healthy Country Flagship Report, CSIRO Land and Water, January 2014, pp.46.

Baatz, M., and A. Schape (2000), Multi-resolution segmentation – an optimization approach for high quality multi-scale segmentation, in Angewandte Geographische Informationsverarbeitung XII, Beiträge zum AGIT Symposium Salsburg 2000, edited by J. Strobl and T. Blaschke, pp. 12-23, Herbert Wichmann Verlag, Salsburg.

Benz, U.C., Hoffman, G., Willhauck, I., Lingenfelder, and Heynen (2004), Multi-resolution, object oriented fuzzy analysis of remote sensing data for GIS ready information. *ISPRS Journal of Photogrammetry & Remote Sensing, 58, 239-258.*

Bernardini , A., Frontoni , E., Malinverni , E. S., Mancini , A.,. Tassetti, A. N, & Zingaretti, P. (2010), Pixel, object and hybrid classification comparisons, *Journal of Spatial Science, 55:1, 43-54*, http://dx.doi.org/10.1080/14498596.2010.487641 .

Borum, J., Duarte, C.M., Krause-Jensen, D. and Greve, T.M. (2004). European seagrasses: an introduction to monitoring and management, The M&MS project, September 2004, Internet version at: http://www.seagrasses.org

Brando, V. E., and A. G. Dekker (2003), Satellite hyperspectral remote sensing for estimating estuarine and coastal water quality, *Geoscience and Remote Sensing, IEEE Transactions on*, *41*(6), 1378-1387.

Boyden, J., Bayliss, P., Kennett, R., Christophersen, P., Lawson, V., McGregor, S. and Begg, G. (2003), Vegetation change analysis on Boggy Plain, South Alligator River, using remote sensing: Report on preliminary analyses. Supervising Scientist Report 430, Supervising Scientist, Department of the Environment and Heritage, Canberra, Australia.

Congalton, R.G. (1991), A Review of Assessing the Accuracy of Classifications of Remotely Sensed Data, *Remote Sensing of the Environment, 37: 35-46*.

Dekker, A. G. , Jordan, A. and Mount, R. (2008). Satellite and airborne imagery including aerial photography. Chapter in "Marine benthic habitat mapping special publication" : p 11-28. Geological Association of Canada: 327 p. ISBN-13: 978-1-897095-33-1; ISSN: 0072-1042.

Dekker, A. G., Brando, V.E., Anstee, J.M., Fyfe, S., Malthus, T.J.M. & Karpouzli, E. (2006), Remote sensing of seagrass ecosystems: use of spaceborne and airborne sensors, Chapter 15 in : Larkum, A,., Orth, B and Duarte, C. (eds) Seagrass Biology, Ecology and Conservation , Springer Verlag, Germany: pp 630.

Duarte, C.M., Alvarez, E., Grau, A. and Krause-Jensen, D. (2004), Which monitoring strategy should be choosen? In: Borum, J., Duarte, C.M., Krause-Jensen, D. and Greve, T.M. (Eds), European seagrasses: an Introduction to monitoring and management, The M&MS project, September 2004, Internet version at: http://www.seagrasses.org

Finlayson, C.M., Bailey, B.J. and Cowie, I.D. (1989) *Macrophyte vegetation of the Magela Creek flood plain, Alligator Rivers Region. Northern Territory*, Supervising Scientist for the Alligator River Region Research Report 5. AGPS, Canberra, pp.38.

Held, A., Byrne, G.T., Anstee, J.M., and Dekker, A. (2003). Determination of SRA Habitat Indicators by Remote Sensing.Technical Report 28/03 CSIRO Land & Water. http://www.clw.csiro.au/publications/technical2003/tr28-03.pdf

Johansen , K., Bartolo, R. & Phinn, S. (2010), SPECIAL FEATURE – Geographic Object-Based Image Analysis, *Journal of Spatial Science, 55:1, 3-7*. http://dx.doi.org/10.1080/14498596.2010.494653

Keppel, G., Van Niel, K. P., Wardell-Johnson, G. W., Yates, C. J., Byrne, M., Mucina, L., Schut, A. G. T., Hopper, S. D. & Franklin, S. E. (2012), Refugia: identifying and understanding safe havens for biodiversity under climate change, Global Ecology and Biogeography, 21(4), 393-404.

Kendrick, G.A., Hegge, B.J., Wyllie, A., Davidson, A., and Lord, D.A. (2000), Changes in seagrass cover on Success and Parmelia Banks, Western Australia between 1965 and 1995. *Estuarine Coastal Shelf Science, 50, 341-353.*

Kirkman, H. (1996), Baseline and monitoring methods for seagrass meadows, *Journal of Environmental Management, 47, 191-201.*

Leguizamon, S., Pelgrum, H. and Azzali, S. (1996), Unsupervised Fuzzy C-Means Classification for the determinations of dynamically Homogeneous Areas, Anais VIII Simpósio Brasileiro de Sensoriamento Remoto, Salvador, Brasil, 14-19 abril 1996, INPE, p. 851-856.

Macleod, R.D. and Congalton, R.G. (1998), A quantitative comparison of change-detection algorithms for monitoring eelgrass from remote sensing data, *Photogrammetry, Engineering and Remote Sensing, 64(3), 207-216.*

TNTMips Pro (2013), MicroImages Inc., Lincoln, Nebraska, USA. http:///www.microimages.com

Ward, D.P., Petty, A., Setterfield, S.A., Douglas, M.M., Ferdinands, K., Hamilton, S., and Phinn, S. (2014), Floodplain inundation and vegetation dynamics in the Alligator Rivers region (Kakadu) of northern Australia assessed using optical and radar remote sensing*. Remote Sensing of Environment 147:43-55.*

Whiteside, T., and R. Bartolo (2014), Vegetation map for Magela Creek floodplain using WorldView-2 multispectral image data.Internal Report 628, April, Supervising Scientist, Darwin.

Appendix A

The interim accuracy assessment tables have been included to illustrate the convolution or combining of the satellite 'classes' so that they could be compared with the broad classes from the helicopter transect data and the more detailed CDU vegetation plot point data. The class labels used in the *in situ* observations are listed in Table 10 and the class labels used in the satellite-derived maps are listed in Table 11.

Table 10 Class labels used for the *in situ* observations

South Alligator video classes	Magela CDU Vegetation Plot measurements	Boggy Plains helicopter video classes
bare ground	aquatic macrophytes	water
Damp, 80 Rice 20 sedge	broad class - *Oryza*/*Eleocharis*/*Nymphaea*/water	water/submerged macrophytes
dry 100 Burn scar, Sen grass/sedge?	*Eleocharis*	grass/sedge - green
Dry, sen grass/sedge 95, 5 BG, Burn scar 100	*Eleocharis*/*Hymenachne*	grass/sedge - green/senescing
grass/sedge	*Hymenachne*	grass/sedge - *Oryza*
grass/sedge - green/senescing	*Hymenachne*/salvinia	grass/sedge - salt tolerant
grass/sedge - *Oryza*	*Leersia*	senescent grass/sedge
grass/sedge - salt tolerant	*Leersia*/*Hymenachne*/ludwigia	*Hymenachne*
Hymenachne	*Leersia*/*Oryza*/*Hymenachne*	
Mangrove	*Leersia*/*Urochloa*/algae	
Melaleuca	mix *Leersia*/*Eleocharis*	
Mudflat/sparse vegetation	*Oryza*	
Mudflat/Water	*Oryza*/algae	
Nymphoidies	*Oryza*/salvinia	
Oryza*/*Leersia	*Psuedoraphis*/salvinia/nymphaea	
***Oryza*/Water**	salvinia/*Eleocharis*	
salt flat/salt tolerant vegetation	sesbania/*Oryza*	
sedge	*Urochloa*	
senescent grass/sedge	*Utricularia*	
sparse vegetation	*Utricularia* /*Nymphaea*	
Water	Water	
water/mangrove	water/*Nelumbo*	
water/submerged macrophytes		

Table 11 Class labels used for the satellite-derived classification

South Alligator ALOS classification	Magela ALOS classification	Boggy Plains 2010 WV2 classification	Boggy Plains 2012 WV2 classification
bare ground	*Eleocharis*	bare ground	bare ground
broad class grass/sedge	Eleocharis sedgelands	broad class - mangrove/Melaleuca	broad class - mangrove/ Melaleuca
broad class grass/sedge/Nelumbo	Hymenachne-Eleocharis	broad class - trees	broad class - trees
Eleocharis dulcis	Leersia	broad class - very green trees	broad class - very green trees
Eleocharis/bare ground	Mangrove/Melaleuca	broad class - Eleocharis/Hymenachne/Nelumbo	Eleocharis
Eleocharis/Psuedoraphis	Melaleuca	Eleocharis	grass/sedge - Hymenachne
Eleocharis/senescing sedge/mud	mixed sedgelands & grasslands	grass/sedge - Eleocharis	Hymenachne
grass/sedge Hymenachne dominated	Nelumbo	grass/sedge - Oryza	Hymenachne/ Nelumbo
grass/sedge Oryza dominated	Oryza	Hymenachne	Melaleuca
grass/sedge salt tolerant	Oryza & Psuedoraphis	Hymenachne/Eleocharis	Nelumbo
Hymenachne acutigluma	Salvinia & Eleocharis	Hymenachne/Nelumbo	senescent grass/sedge
Mangrove		Melaleuca	sparse vegetation
Mangrove/Eleocharis		Nelumbo	water
Melaleuca		Nelumbo/bare ground	water/submerged macrophytes
Melaleuca/Mangrove		senescent grass/sedge	Woodland
mix		sparse vegetation	
Eleocharis/Nelumbo/Hymenachne/open water		Water	
mudflat		Woodland	
mudflat/sparse vegetation			
mudflat/water			
Nelumbo/Hymenachne			
Nelumbo/Nymphaea/Nymphoides			
Oryza meriondalis			
Oryza/Eleocharis			
salt flat/salt tolerant vegetation			
unresolved trees			
water			
woodland			

A.1 The South Alligator River floodplain ALOS classification accuracy

The South Alligator ALOS classification accuracy assessment (in pixels), helicopter video transect data (columns) vs satellite classification (rows) – for readability split in 2 sections.

	bareground + dry, sen grass	Damp, 80 Rice 20 sedge	Dry, sen grass/sedge 95, 5 BG	grass/sedge	grass/sedge - green/senescing	grass/sedge - oyrza	grass/sedge salt tolerant	hymenachne	mangrove	melaleuca	mudflat/sparse vegetation
bare ground	55	0	1	0	35	185	328	803	0	0	0
broad class grass/sedge	0	0	177	0	2	0	0	42	0	0	0
broad class grass/sedge/Nelumbo	0	0	0	0	0	0	0	0	6	0	0
Eleocharis dulcis	0	0	0	0	0	0	0	0	0	0	0
Eleocharis/bare ground	31	0	0	0	0	0	115	0	0	0	0
Eleocharis/Psuedoraphis	123	0	45	0	3	0	4	0	0	0	0
Eleocharis/senescing sedge/mud	506	0	1	0	0	0	1524	0	0	0	326
grass/sedge Hymenachne dominated	0	0	0	0	0	0	0	0	0	0	0
grass/sedge Oryza dominated	2704	8	367	0	6301	499	10068	152	0	0	0
grass/sedge salt tolerant	0	0	0	330	9241	0	2441	0	0	417	4
Hymenachne acutigluma	0	0	0	0	0	15	0	6	0	0	0
Mangrove	0	0	5	76	45	0	19	428	465	22	0
Mangrove/eleocharis	0	0	0	0	0	0	0	0	0	0	0
Melaleuca	0	0	0	0	124	0	12	49	0	170	0
Melaleuca/Mangrove	0	0	0	0	44	0	8	12	0	25	0
mix Eleocharis/Nelumbo/Hymenachne/water	0	0	0	0	0	0	0	0	31	0	0
mudflat	30	0	0	0	3	231	1	0	2	0	4
mudflat/sparse vegetation	0	0	0	0	0	0	0	146	0	0	0
mudflat/water	0	0	7	0	0	0	218	0	3164	0	43
Nelumbo/Hymenachne	0	0	0	0	0	0	0	47	0	0	0
Nelumbo/Nymphaea/Nymphoides	0	0	0	0	0	0	0	0	12	0	0
Oryza meriondalis	3887	197	64	0	346	139	5802	635	0	0	0
Oryza/Eleocharis	7	29	60	5	2746	3	9089	231	0	11	68
salt flat/salt tolerant vegetation	0	0	0	0	386	48	1960	0	1	0	3588
unresolved trees	0	0	0	0	0	0	0	1	0	0	0
water	83	0	409	4	40	0	843	0	48	2	4
woodland	0	0	0	0	1	0	2	0	0	0	0
sum	7426	234	1136	415	19317	1120	32434	2552	3729	647	4037

	mudflat/water	nymphoides	oryza/leersia	oryza/water	salt flat/salt tolerant vegetation	sedge	senescent grass/sedge	sparse vegetation	water	water/mangrove	water/submerged macrophytes		
bare ground	300	0	3	6	366	0	799	79	0	0	27		1580
broad class grass/sedge	3	0	0	48	0	0	177	0	0	0	425		653
broad class grass/sedge/Nelumbo	0	0	0	0	0	0	0	0	5	0	0		5
Eleocharis dulcis	0	418	0	0	0	0	0	0	0	0	0		418
Eleocharis/bare ground	0	22	0	0	0	0	23	0	0	0	0		45
Eleocharis/Psuedoraphis	0	1	0	0	0	0	14	3	0	0	0		18
Eleocharis/senescing sedge/mud	0	0	0	0	76	0	90	9	0	0	0		175
grass/sedge Hymenachne dominated	0	2031	0	0	0	0	0	0	0	0	0		2031
grass/sedge Oryza dominated	60	0	0	0	20	93	20170	2325	0	0	0		22668
grass/sedge salt tolerant	11	0	52	0	97	0	5475	0	0	0	0		5635
Hymenachne acutigluma	0	0	0	0	0	0	0	0	0	0	0		0
Mangrove	23	2	251	1	0	4	26	0	0	0	0		307
Mangrove/eleocharis	0	1	0	8	0	0	0	0	0	0	0		9
Melaleuca	42	0	0	2	0	1	238	0	0	0	0		283
Melaleuca/Mangrove	5	0	0	11	0	7	48	3	0	0	0		74
mix Eleocharis/Nelumbo/Hymenachne/water	0	0	0	0	0	0	0	0	16	0	0		16
mudflat	0	0	0	0	0	0	29	0	0	0	0		29
mudflat/sparse vegetation	0	0	0	2362	0	0	11	0	0	0	5		2378
mudflat/water	0	0	0	0	0	0	1	0	57035	7680	0		64716
Nelumbo/Hymenachne	1	0	0	69	0	0	15	0	0	0	3		88
Nelumbo/Nymphaea/Nymphoides	0	0	0	0	0	0	0	0	0	0	0		0
Oryza meriondalis	0	0	0	0	5	390	6970	196	0	0	0		7561
Oryza/Eleocharis	2158	o	567	0	6192	0	17564	72	0	0	0		26553
salt flat/salt tolerant vegetation	0	0	0	0	1687	0	925	8	0	0	0		2620
unresolved trees	0	0	0	2	0	0	13	0	0	0	0		15
water	0	0	691	0	0	12	50	0	46	0	0		799
woodland	2	0	0	0	0	0	101	0	0	0	0		103
sum	2605	2475	1564	2509	8443	507	52739	2695	57102	7680	460		138779

Combining classes:

	bare ground	grass/sedge senescing	Eleocharis	nelumbo	oryza	salt tolerant vegetation	trees	water or mudflats	row total
bare ground	55	80	0	27	1028	694	0	300	1884
grass/sedge senescing	0	177	0	425	227	0	6	8	835
Eleocharis	660	185	0	0	130	1719	37	326	2731
nelumbo	0	0	0	0	84	0	12	1	96
oryza	3887	591	0	0	35369	31176	11	2286	71034
salt tolerant vegetation	2711	2756	0	0	16127	6185	418	3603	28197
trees	83	81	0	0	745	41	682	70	1632
water or mudflats	30	65232	0	0	3418	1062	3216	64812	72958
column total	7426	69102	0	452	57128	40877	4382	71406	250773
kappa	0.42779	0.42769	0.4278	0.4278	0.4088	0.42549	0.42777	0.38234	
tau	0.4278	0.4278	0.4278	0.4278	0.40399	0.42621	0.42779	0.38127	

OVERALL ACCURACY = 42.7%

	bare ground	Nelumbo/grass/sedge senescing	oryza/salt tolerant vegetation	trees	water or mudflats	row total
bare ground	55	107	1722	0	300	2184
Nelumbo/grass/sedge senescing	660	787	2160	55	335	3997
oryza/salt tolerant vegetation	6598	3347	88857	429	5889	105120
trees	83	81	786	682	70	1702
water or mudflats	30	65232	4480	3216	64812	137770
column total	7426	69554	98005	4382	71406	250773
kappa	0.42779	0.4273	0.33582	0.42777	0.38234	

OVERALL ACCURACY = 61.9%

Further combining:

	Nelumbo/Eleocharis/grass/sedge senescing	oryza/salt tolerant vegetation	trees	water or mudflats	row total
Nelumbo/Eleocharis/grass/sedge senescing	787	2160	55	335	3337
oryza/salt tolerant vegetation	3347	88857	429	5889	98522
trees	81	786	682	70	1619
water or mudflats	65232	4480	3216	64812	137740
column total	69447	96283	4382	71106	241218
kappa	0.44422	0.34903	0.44471	0.39698	
tau	0.42777	0.32646	0.42779	0.3241	

OVERALL ACCURACY = 64.3%

A.2 The Magela floodplain ALOS classification accuracy

The Magela ALOS classification accuracy assessment (in pixels), permanent vegetation plot observations (columns) vs satellite classification (rows) – for readability split in 2 sections.

	aquatic macrophytes	broad class - oryza/eleocharis/ nymphaea/water	eleocharis	eleocharis/hymenachne	hymenachne	hymenachne/salvinia	leersia	leersia/hymenachne/ludwigia	leersia/oryza/hymenachne	leersia/urochloa/ algae	mix leersia/eleocharis
Eleocharis	0	6	68	0	30	0	0	0	0	0	0
hymenachne	12	0	0	0	0	0	46	0	2	24	0
Hymenachne-Eleocharis	0	0	0	36	0	0	26	34	20	0	0
Leersia	0	4	0	0	24	0	169	0	0	0	16
mangrove/melaleuca	0	0	0	0	0	0	1	0	0	0	0
Melaleuca	0	0	2	0	0	0	10	0	0	0	10
mix sedgelands & grasslands	0	0	12	0	8	0	110	2	0	18	0
nelumbo	0	0	0	0	0	0	0	0	0	0	0
oryza	24	0	30	0	14	57	46	0	14	0	0
oryza & psuedoraphis	0	28	135	0	0	0	78	0	0	0	0
salvinia/eleocharis	0	0	0	0	0	0	0	0	0	0	0
sum	36	38	247	36	76	57	486	36	36	42	26

	oryza	oryza/algae	oryza/salvinia	psuedoraphis/salvinia/nymphaea	salvinia/eleocharis	sesbania/oryza	urochloa	utricularia	utricularia/nymphaea	water	water/nelumbo	no of classified pixels
Eleocharis	3	0	0	0	0	0	63	0	0	0	60	230
hymenachne	0	30	38	0	0	0	92	0	8	0	0	252
Hymenachne-Eleocharis	0	0	0	0	0	0	10	0	8	0	0	134
Leersia	14	0	0	0	0	0	42	0	24	0	0	293
mangrove/melaleuca	0	0	0	0	0	1	1	0	0	0	0	3
Melaleuca	9	0	0	0	0	4	2	0	0	0	0	37
mix sedgelands & grasslands	132	12	0	0	0	30	32	42	0	38	36	472
nelumbo	0	0	0	0	0	0	16	0	0	0	2	18
oryza	84	0	0	0	14	0	46	0	30	0	4	363
oryza & psuedoraphis	20	0	0	40	0	0	38	10	0	0	0	349
salvinia/eleocharis	0	0	0	0	22	0	0	0	0	0	0	22
sum	262	42	38	40	36	35	342	52	70	38	102	2173

By combining classes:

	Eleocharis	Hymenachne	Leersia	mixed sedgelands and grasslands	nelumbo	oryza	oryza & psuedoraphis	salvinia/eleocharis	urochloa	utricularia		row total
Eleocharis	104	30	26	0	60	23	135	0	73	8		459
Hymenachne	0	0	46	54	0	2	0	0	92	8		202
Leersia	0	24	169	0	0	14	78	0	42	24		351
mix sedgelands & grasslands	12	8	110	60	36	132	0	0	32	42		432
nelumbo	0	0	0	0	2	0	0	0	16	0		18
oryza	30	71	46	0	4	98	20	14	46	30		359
oryza & psuedoraphis	135	0	78	0	0	20	40	0	38	10		321
salvinia/eleocharis	0	0	0	0	0	0	0	22	0	0		22
urochloa	0	0	0	0	0	0	0	0	0	0		0
utricularia	0	0	0	0	0	0	0	0	0	0		0
column total	281	133	475	114	102	289	273	36	339	122		2164
kappa	0.2239	0.228743	0.215291	0.227615	0.228709	0.22405	0.22694	0.228613	0.228743	0.228743		
tau	0.2208	0.228743	0.215752	0.22418	0.228592	0.221263	0.225707	0.227076	0.228743	0.228743		

OVERALL ACCURACY = 22.8%

Combining Urochloa and Utricularia in with sedge/grasslands:

	Eleocharis	Hymenachne	Leersia	mixed sedgelands and grasslands	nelumbo	oryza	oryza & psuedoraphis	salvinia/eleocharis
Eleocharis	104	30	26	63	60	23	135	0
Hymenachne	0	0	46	154	0	2	0	0
Leersia	0	24	169	66	0	14	78	0
mixed sedgelands and grasslanc	12	8	110	134	36	132	0	0
nelumbo	0	0	0	16	2	0	0	0
oryza	30	71	46	76	4	98	20	14
oryza & psuedoraphis	135	0	78	48	0	20	40	0
salvinia/eleocharis	0	0	0	0	0	0	0	22
column total	281	133	475	557	102	289	273	36
kappa	0.2239	0.228743	0.215291	0.216251	0.228709	0.22405	0.22694	0.228613
tau	0.2208	0.228743	0.215752	0.218478	0.228592	0.221263	0.225707	0.227076

OVERALL ACCURACY = 26.5%

Combining *Leersia*, *Urochloa* and Iutricularia in with sedge/grasslands:

	Eleocharis	Hymenachne	mixed sedgelands and grasslands	nelumbo	oryza		row total
Eleocharis	126	30	89	60	158		463
Hymenachne	0	0	200	0	2		202
mixed sedgelands and grasslanc	12	32	479	36	224		783
nelumbo	0	0	16	2	0		18
oryza	179	71	248	4	178		680
column total	317	133	1032	102	562		2146
kappa	0.222108	0.228743	0.137721	0.228709	0.211908		
tau	0.219099	0.228743	0.190749	0.228592	0.215048		

OVERALL ACCURACY = 36.6%

A.3 The 2010 Boggy Plain WV2 classification accuracy assessment

The 2010 Boggy Plain WV2 classification accuracy assessment (in pixels), helicopter video transect data (columns) vs satellite classification (rows).

	water	grass/sedge - green	grass/sedge - green/senescing	grass/sedge - oryza	grass/sedge - salt tolerant	senescent grass/sedge	hymenachne	water/submerged macrophytes	no. Classified pixels
bare ground	1244	6	11385	0	1185	55141	0	0	68961
broad class - mangrove/melaleuca	734	300	0	0	22	0	275	0	1331
broad class - trees	512	161	0	0	12	0	159	0	844
broad class - very green trees	55	0	0	0	0	0	0	0	55
broad class -eleocharis/hymenachne/nelumbo	0	0	0	0	0	0	156	77	233
Eleocharis	1	0	901	6	482	303	4	0	1697
grass/sedge - eleocharis	0	235	118	112	901	68	968	0	2402
grass/sedge - oryza	0	1462	12763	8726	0	832	1800	0	25583
Hymenachne	19	0	16	2359	0	0	16193	459	19046
hymenachne/eleocharis	0	0	0	2320	0	0	2504	1	4825
hymenachne/nelumbo	25	0	0	0	0	0	2322	8513	10860
Melaleuca	216	0	221	0	8	0	47	0	492
Nelumbo	11	0	0	0	0	0	6	2333	2350
nelumbo/bare ground	0	0	105	12	73	0	383	0	573
senescent grass/sedge	1	138	1608	60	20	9810	268	0	11905
sparse vegetation	0	61	12667	0	236	54542	13	0	67519
Water	100961	0	0	0	0	0	0	103	101064
Woodland	19	0	413	0	8	4	9	0	453
no. ground truth pixels	103798	2363	40197	13595	2947	120700	25107	11486	320193

By combining classes:

	Eleocharis	Hymenachne	grass/sedge - oryza	nelumbo	senescent grass/sedge	water		row total
Eleocharis	0	0	0	0	0	0		0
Hymenachne	0	21175	4695	9050	16	44		34980
grass/sedge - oryza		1800	10188	0	13595	0		25583
nelumbo	0	53	12	0	178	11		254
senescent grass/sedge	0	281	259	0	78883	1		79424
water	0	0	0	103	0	100961		101064
column total	0	23309	15154	9153	92672	101017		241305
kappa	0	0.874204	0.874938	0.87527	0.857362	0.848784		
tau	0	0.873663	0.874709	0.87527	0.860231	0.848769		

OVERALL ACCURACY = 87.5%

A.4 The 2012 Boggy Plain WV2 classification accuracy assessment

The 2012 Boggy Plain WV2 classification accuracy assessment (in pixels), helicopter video transect data (columns) vs satellite classification (rows).

	grass/sedge - green	grass/sedge - green/senescing	grass/sedge - oryza	grass/sedge - salt tolerant	senescent grass/sedge	hymenachne	water	water/submerged macrophytes		row total
bare ground	49	7734	2279	3273	4148	226	3	0		17712
broad class - mangrove/melaleuca	0	263	0	47	0	286	517	0		1113
broad class - trees	0	8	0	1	0	7	334	0		350
broad class - very green trees	0	0	0	0	0	1	390	0		391
Eleocharis	261	5091	6323	15	5304	39689	17	391		57091
grass/sedge - hymenachne	0	0	0	0	0	6167	21	701		6889
Hymenachne	0	0	0	0	0	665	12	9566		10243
hymenachne/nelumbo	0	0	0	0	0	2799	63	800		3662
Melaleuca	0	751	0	5	2	0	171	0		929
nelumbo	0	0	0	0	0	90	34	28		152
senescent grass/sedge	4364	54546	11904	12487	88995	480	0	0		172776
sparse vegetation	12588	59395	127	20412	110686	24	0	0		203232
water	20	42	1231	1	18	31	101725	0		103068
water/submerged macrophytes	0	0	0	0	0	0	14	0		14
Woodland	0	72	0	0	0	41	145	0		258
sum	17282	127902	21864	36241	209153	50506	103446	11486		577880

By combining the above classes:

	Eleocharis	Hymenachne	nelumbo	senescent grass/sedge	water		row total
Eleocharis	0	39689	0	0	0		39689
Hymenachne	0	6832	1092	16994	38		24956
nelumbo	0	2889	828	0	97		3814
senescent grass/sedge	0	504	0	375504	0		376008
water	0	31	0	1312	101725		103068
column total	0	49945	1920	393810	101860		547535
kappa	0.885585	0.885455	0.885585	0.774214	0.881489		
tau	0.885585	0.88552	0.885584	0.78373	0.884024		

OVERALL ACCURACY = 88.6%

A.5 Data repository

The following data products generated by this project can be obtained from the CSIRO Data Access Portal using the specified URLs.

Kakadu floodplain vegetation maps (ArcGIS map packages)

https://data.csiro.au/dap/landingpage?pid=csiro:9107

Kakadu LiDAR Project 2011 0.5m Contours maps

http://hdl.handle.net/102.100.100/13883?index=1

Kakadu LiDAR Intensity Mosaic (ECW format)

http://dx.doi.org/10.4225/08/547CFAED7DB89

Kakadu LiDAR Classified point clouds AHD

http://dx.doi.org/10.4225/08/54770ECCD1F66

Kakadu LiDAR Classified point clouds ELL

http://hdl.handle.net/102.100.100/13881?index=1

Kakadu LiDAR Unclassified point clouds ELL

http://hdl.handle.net/102.100.100/13882?index=1

Kakadu LiDAR (1 metre) Digital Elevation Model (DEM) (tiled)

http://dx.doi.org/10.4225/08/547CFABF81E84

Kakadu LiDAR (1 metre) Digital Surface Model (DSM) (tiled)

http://dx.doi.org/10.4225/08/547CFAD851A9C

Kakadu LiDAR (2 metre) Canopy Height Model (CHM)

http://hdl.handle.net/102.100.100/13879?index=1

Kakadu LiDAR (10 metre) Forest Canopy Model (FCM)

http://hdl.handle.net/102.100.100/13878?index=1

CONTACT US

t 1300 363 400
+61 3 9545 2176
e enquiries@csiro.au
w www.csiro.au

YOUR CSIRO

Australia is founding its future on science and innovation. Its national science agency, CSIRO, is a powerhouse of ideas, technologies and skills for building prosperity, growth, health and sustainability. It serves governments, industries, business and communities across the nation.

FOR FURTHER INFORMATION

CSIRO Oceans and Atmosphere Flagship
Janet Anstee
t +61 2 6246 5714
e janet.anstee@csiro.au
w www.csiro.au/businessunit-flagshipname